Robotica (2008) volume 26, pp. 587–599. © 2008 Cambridge University Press
doi:10.1017/S0263574708004165 Printed in the United Kingdom

Kinematic models and isotropy analysis of wheeled mobile robots

Luis Gracia* and Josep Tornero

Dept. of Systems Engineering and Control, Technical University of Valencia, P.O. Box: 22012, E-46071, Valencia (Spain)

(Received in Final Form: December 29, 2007. First published online: February 19, 2008)

SUMMARY

This research presents a comprehensive and useful survey of the kinematic models of wheeled mobile robots and their optimal configurations. The kinematic modeling of wheeled mobile robots with no-slip is presented, by considering four common types of wheels: *fixed*, *orientable*, *castor,* and *Swedish*. Next, the accuracy of the kinematic models is discussed considering their sensitivity or relative error amplification, giving rise to the isotropy concept. As practical application of the previous theory, all types of three-wheeled mobile robots are modeled and their optimal (isotropic) configurations for no error amplification are obtained. Finally, three practical examples of error amplification are developed for several types of wheeled mobile robots in order to illustrate the benefits and limitations of the isotropic configurations.

KEYWORDS: Model accuracy; Isotropy; Optimal configurations; Wheeled mobile robots.

1. Introduction

Wheeled Mobile Robots (WMRs) have been widely studied in the past fifteen years. Due to kinematic constraints, many WMRs are not integrable (non-holonomic) and therefore standard techniques developed for robot manipulators are not directly applicable. Modeling, which is often a prerequisite to control design and motion planning, is however still a relevant issue. Examples of WMR kinematic models are available in the literature,[1–6] although not all of them employ a systematic procedure. On the other hand, the *sensitivity* (relative error amplification) of the WMR kinematic models should be minimized. In this sense, for some special configurations *isotropy* is achieved and there is no error amplification.[5] Therefore, the aim of this research is to give a wide survey of the kinematic models of WMR, their isotropy conditions, and the benefits and limitations of isotropy.

The paper is organized as follows. Section 2 presents the kinematic modeling of a WMR with no slip by considering four types of wheels: *fixed*, centered orientable (hereinafter *orientable*), off-centered orientable or *castor,* and *Swedish*. This section also discusses the accuracy of the kinematic models and introduces the isotropy concept. As practical application of Section 2, Section 3 generates the kinematic models for the five types of WMRs, classified according to Campion *et al.*,[1] and obtains all their isotropy conditions, i.e. the optimal configurations for no relative error amplification.

* Corresponding author. E-mail: luigraca@isa.upv.es

Afterwards, Section 4 shows three practical examples of error amplification for several types of mobile robots in order to illustrate the benefits and limitations of isotropy. Finally, Section 5, points out the more outstanding contributions of this research and suggests future works.

2. Kinematic Modeling of Wheeled Mobile Robots with No Slip

Firstly it will be introduced some terminology. Assuming horizontal movement, the position of the WMR body is completely specified by 3 scalar variables (e.g. x, y, θ), referred[1] as WMR posture, $\mathbf{p}$ in vector form. Its first-order time derivative is called[2] WMR velocity vector $\dot{\mathbf{p}}$ and separately (v_x, v_y, ω) WMR velocities. Similarly, for each wheel, wheel velocity vector and wheel velocities are defined.[2]

2.1. Kinematic models of the four common types wheels

The kinematic modeling of a wheel is used as a previous stage for modeling the whole WMR.[1–4] Here, the four common wheels will be considered: *fixed*, *orientable*, *castor,* and *Swedish*. As it is easy to obtain their equations using a vector approach, e.g. see Gracia and Tornero[4] among many other possibilities, the detailed development will be omitted.

The matrix equation of the *castor* wheel is:

$$\mathbf{v}_{\text{slip}\,i} = \begin{pmatrix} \cos(\beta_i+\delta_i) & \sin(\beta_i+\delta_i) & & \\ -\sin(\beta_i+\delta_i) & \cos(\beta_i+\delta_i) & & \\ \mathrm{l}_i\sin(\beta_i+\delta_i-\alpha_i)-\mathrm{d}_i\cos\delta_i & -\mathrm{d}_i\cos\delta_i & 0 \\ \mathrm{l}_i\cos(\beta_i+\delta_i-\alpha_i)+\mathrm{d}_i\sin\delta_i & \mathrm{d}_i\sin\delta_i & \mathrm{r}_i \end{pmatrix} \times \begin{pmatrix} \dot{\mathbf{p}} \\ \dot{\beta}_i \\ \dot{\varphi}_i \end{pmatrix}, \tag{1}$$

where it has been used the parameters of Fig. 1 and the variables of Table I. The equation of the *orientable* wheel can be obtained from (1) with $\mathrm{d}_i = \delta_i = 0$:

$$\mathbf{v}_{\text{slip}\,i} = \begin{pmatrix} \cos\beta_i & \sin\beta_i & \mathrm{l}_i\sin(\beta_i-\alpha_i) & 0 \\ -\sin\beta_i & \cos\beta_i & \mathrm{l}_i\cos(\beta_i-\alpha_i) & \mathrm{r}_i \end{pmatrix} \begin{pmatrix} \dot{\mathbf{p}} \\ \dot{\varphi}_i \end{pmatrix}, \tag{2}$$

which is also valid for *fixed* wheels, where the angle β_i is constant. The matrix equation of the *Swedish* wheel, see Fig. 2(a), is (3) where the parameters of Fig. 2(b) and the

TABLE I-Frames, variables and constants.

Symbol	Description
R	Frame attached to the robot body with the Z-axis perpendicular to the floor surface
$\bar{\mathrm{R}}$	Frame attached to the floor and instantaneously coincident with the robot frame R. This frame allows to avoid the dependency on a global stationary frame[2]
$(\mathrm{L}_i, \mathrm{E}_i)$	Frames attached to the wheel i and to the roller of the *Swedish* wheel i, with the X-axes coincident with their rotation axle
$\dot{\mathbf{p}}$	WMR velocity vector in coordinate frame $\bar{\mathrm{R}}$, equivalent to $({}^{\bar{\mathrm{R}}}v_{\mathrm{R}x}\ {}^{\bar{\mathrm{R}}}v_{\mathrm{R}y}\ {}^{\bar{\mathrm{R}}}\omega_{\mathrm{R}})^{\mathrm{T}}$ or $(v_x\ v_y\ \omega)^{\mathrm{T}}$
$\mathbf{v}_{\mathrm{slip}\,i}$	Sliding velocity vector of the wheel in coordinate frame L_i (E_i for *Swedish* wheels)
$(\dot{\beta}_i, \dot{\varphi}_i)$	Angular velocity of the steering link and rotation velocity of the wheel in L_{xi}-axis
$\dot{\varphi}_{ri}$	Rotation velocity of the rollers in E_{xi}-axis (it is usually a free wheel velocity)
$(\mathrm{r}_i, \mathrm{r}_{ri})$	Wheel equivalent radius and roller radius.

variables and constants of Table I have been used.

$$\mathbf{v}_{\mathrm{slip}\,i} = \begin{pmatrix} \cos(\beta_i+\gamma_i) & \sin(\beta_i+\gamma_i) \\ -\sin(\beta_i+\gamma_i) & \cos(\beta_i+\gamma_i) \end{pmatrix} \begin{pmatrix} \mathrm{l}_i \sin(\beta_i+\gamma_i-\alpha_i) & \mathrm{r}_i \sin\gamma_i & 0 \\ \mathrm{l}_i \cos(\beta_i+\gamma_i-\alpha_i) & \mathrm{r}_i \cos\gamma_i & \mathrm{r}_{ri} \end{pmatrix} \begin{pmatrix} \dot{\mathbf{p}} \\ \dot{\varphi}_i \\ \dot{\varphi}_{\mathrm{r}\,i} \end{pmatrix} \tag{3}$$

2.2. Composite equation and kinematic model with no slip

Once the type of WMR wheels and their equations are established, a compound kinematic equation for the WMR may be defined. By virtue of (1), (2), and (3), we have:

$$\mathbf{v}_{\mathrm{slip}} = \begin{pmatrix} \mathbf{v}_{\mathrm{slip}\,1} \\ \vdots \\ \mathbf{v}_{\mathrm{slip}\,\mathrm{N}} \end{pmatrix} = \begin{pmatrix} \mathbf{A}_{\mathrm{p}1} & \mathbf{A}_{\mathrm{w}1} & \cdots & 0 \\ \vdots & \vdots & \ddots & \vdots \\ \mathbf{A}_{\mathrm{pN}} & 0 & \cdots & \mathbf{A}_{\mathrm{wN}} \end{pmatrix} \begin{pmatrix} \dot{\mathbf{p}} \\ \dot{\mathbf{q}}_{\mathrm{w}1} \\ \vdots \\ \dot{\mathbf{q}}_{\mathrm{wN}} \end{pmatrix} \tag{4}$$

$$\mathbf{v}_{\mathrm{slip}} = (\mathbf{A}_{\mathrm{p}}\ \mathbf{A}_{\mathrm{w}}) \begin{pmatrix} \dot{\mathbf{p}} \\ \dot{\mathbf{q}}_{\mathrm{w}} \end{pmatrix} = \mathbf{A}\,\dot{\mathbf{q}},$$

where N is the number of wheels; $\mathbf{v}_{\mathrm{slip}}$ is the composite sliding velocity vector; $\dot{\mathbf{q}}_{\mathrm{w}i}$ is a vector with all the wheel velocities of wheel i; $\dot{\mathbf{q}}_{\mathrm{w}}$ is the composite vector of all the wheel velocities; $\dot{\mathbf{q}}$ is the vector of all the wheel and WMR velocities; $\{\mathbf{A}_{\mathrm{p}i}, \mathbf{A}_{\mathrm{w}i}\}$ are the multiplying matrices obtained from (1), (2), and (3); $\{\mathbf{A}_{\mathrm{p}}, \mathbf{A}_{\mathrm{w}}\}$ are the composite matrices; and $\mathbf{A}$ is the WMR kinematic matrix. Under the *no-slip condition*, the kinematic solution for velocity vector $\dot{\mathbf{q}}$ results:

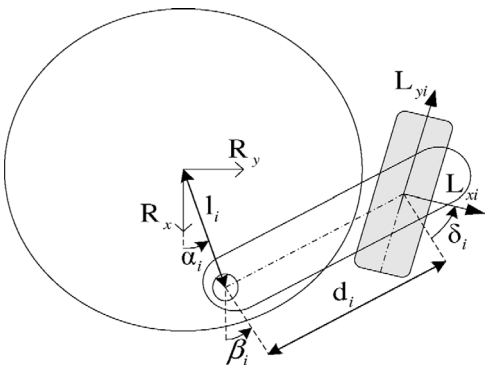

Fig. 1. *Castor* wheel parameters: $\mathrm{l}_i, \mathrm{d}_i, \alpha_i, \beta_i, \delta_i$.

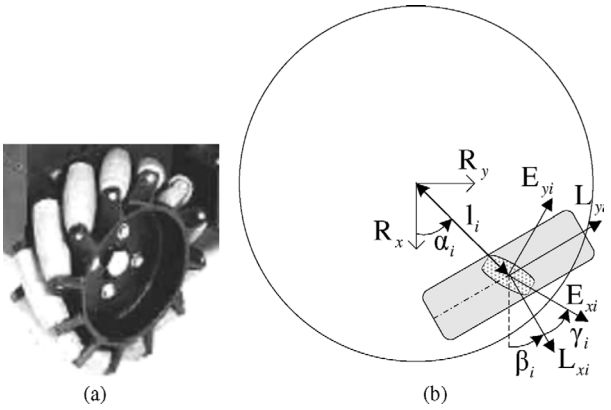

Fig. 2. (a) *Swedish* wheel (or *Mecanum* or *universal*) with rollers at 45°. (b) Parameters of the Swedish wheel: $\mathrm{l}_i, \alpha_i, \beta_i, \gamma_i$.

$$\mathbf{A} \cdot \dot{\mathbf{q}} = \mathbf{0} \tag{5}$$

$$\dot{\mathbf{q}} \in \mathcal{N}(\mathbf{A}) \rightarrow \dot{\mathbf{q}} = \mathbf{B} \cdot \boldsymbol{\eta}, \tag{6}$$

where matrix $\mathbf{B}$ forms a basis of $\mathcal{N}(\mathbf{A})$, $\boldsymbol{\eta}$ is an m-dimensional vector representing WMR mobility, m is the WMR mobility degree given by the *nullity* of $\mathbf{A}$ (see the *rank-nullity* theorem):

$$m = \dim(\boldsymbol{\eta}) = \dim(\mathcal{N}(\mathbf{A})) = \dim(\dot{\mathbf{q}}) - \mathrm{rank}(\mathbf{A}) = k - g. \tag{7}$$

In order to use variables with physical meaning, the mobility vector $\boldsymbol{\eta}$ should be replaced with a set of freely *assigned* velocities. Depending on whether wheel velocities or WMR velocities are chosen, a forward or inverse kinematic model is obtained. If a mix of both types of velocities is chosen a mixed solution is achieved. In order to check if an m-set of velocities $\dot{\mathbf{q}}_{\mathrm{a}}$ can be assigned, it must be verified that the determinant of the submatrix $\mathbf{B}_{\mathrm{a}}$ that they define in (6) is non zero, that is:

$$\begin{pmatrix} \dot{\mathbf{q}}_{\mathrm{na}} \\ \dot{\mathbf{q}}_{\mathrm{a}} \end{pmatrix} = \begin{pmatrix} \mathbf{B}_{\mathrm{na}} \\ \mathbf{B}_{\mathrm{a}} \end{pmatrix} \cdot \boldsymbol{\eta} \tag{8}$$

$$\text{if } |\mathbf{B}_{\mathrm{a}}| \neq 0 \ \rightarrow\ \dot{\mathbf{q}}_{\mathrm{na}} = \mathbf{B}_{\mathrm{na}} \cdot \mathbf{B}_{\mathrm{a}}^{-1} \cdot \dot{\mathbf{q}}_{\mathrm{a}}, \tag{9}$$

where $\dot{\mathbf{q}}_{\mathrm{na}}$ are the remaining non-assigned velocities of $\dot{\mathbf{q}}$.

2.3. Accuracy of the kinematic models: isotropy

The accuracy of the forward and inverse kinematics, when an input data error is considered, has been studied by several authors through the characterization of isotropic matrices. For instance, Saha et al.[5] established the isotropy conditions for a generic WMR with *Swedish* wheels, and specified them when using three and four wheels. While, Low and

https://doi.org/10.1017/S0263574708004165 Published online by Cambridge University Press

Leow[6] and Kim *et al.*[7–9] studied the isotropy conditions for an omnidirectional WMR with three *castor* wheels. Here, isotropy is studied by the following algebraic equation:

$$\mathbf{H}\mathbf{x} = \mathbf{y}, \tag{10}$$

where $\mathbf{x}$ is the n'-dimensional output (unknown) variable vector, $\mathbf{y}$ is the n-dimensional input (known) data vector, and $\mathbf{H}$ is an $n \times n'$-dimensional matrix. A precise measure of the *sensitivity* of the linear system can be obtained by considering the parameterized system:

$$(\mathbf{H} + \in \mathbf{F})\,\mathbf{x}(\in) = \mathbf{y} + \in \mathbf{f}, \tag{11}$$

where $\in$ is the error parameter and $\{\in \mathbf{F}, \in \mathbf{f}\}$ the input data errors. In case $n = n'$, using any vector norm and consistent matrix norm it is obtained[10]:

$$\begin{aligned} &\frac{\|\mathbf{x}(\in) - \mathbf{x}\|}{\|\mathbf{x}\|} \le \kappa(\mathbf{H}) \left(|\in| \frac{\|\mathbf{F}\|}{\|\mathbf{H}\|} + |\in| \frac{\|\mathbf{f}\|}{\|\mathbf{y}\|} \right) O(\in^2) \\ &\rho_{\mathbf{x}} \le \kappa(\mathbf{H})(\rho_{\mathbf{H}} + \rho_{\mathbf{y}}) + O(\in^2), \end{aligned} \tag{12}$$

where $\kappa(\cdot)$ is the condition number of a matrix; $\{\rho_{\mathbf{H}}, \rho_{\mathbf{y}}\}$ are the relative errors of the input data; $\rho_{\mathbf{x}}$ is the relative error of the output vector; and $O(\in^2)$ is the Taylor series expansion of $\mathbf{x}(\in)$ beginning from the second-order term. It is interesting to remark that $O(\in^2)$ is *null* if $\mathbf{F} = \mathbf{0}$. Otherwise, it *can be neglected* if the parameter error $\in$ is small.

It is stated[5–11] that the condition number of $\mathbf{H}$ matrix is a measurement of the relative error *amplification* of the computed results $\mathbf{x}$ (with left pseudo-inverse if $n > n'$ and with right pseudo-inverse if $n < n'$) with respect to the relative error of the input data $\{\mathbf{H}, \mathbf{y}\}$. When the condition number is equal to unity (i.e. $\mathbf{H}$ is isotropic) no error amplification is obtained, which is the best possible situation.

Certainly, it can bee seen in (12) that the condition number of $\mathbf{H}$ is a *proportionality* measure of the *maximum* error amplification as long as $O(\in^2)$ is null or negligible. In fact, this maximum error amplification will be achieved only for specific values of $\{\mathbf{H}, \mathbf{y}, \mathbf{F}, \mathbf{f}\}$. This important remark, κ $(\mathbf{H})$ represents an *upper bound* as long as $O(\in^2)$ is *negligible*, has been usually omitted[5–9] although it may be very influential in practice, as it is illustrated in the examples of Section 4.

By using the Euclidean norm, the condition number of a matrix is:

$$\kappa_2(\mathbf{H}) = \|\mathbf{H}\|_2 \left\|\mathbf{H}^*\right\|_2 = \sigma_l/\sigma_s \to \kappa_2(\cdot) \in [1, \infty], \tag{13}$$

where supra-index * denotes the conjugate transpose matrix and $\{\sigma_l, \sigma_s\}$ are the largest and smallest singular values of matrix $\mathbf{H}$. Thus, singular matrices (σ_s is zero) have an infinitely large condition number. If $\mathbf{H}$ is isotropic the following equation is satisfied:

$$\text{if } n > n' \quad \mathbf{H}^{\mathrm{T}}\mathbf{H} = \mathrm{k}\mathbf{I} \quad \text{else} \quad \mathbf{H}\mathbf{H}^{\mathrm{T}} = \mathrm{k}\mathbf{I}, \tag{14}$$

where k is a proportionality constant and $\mathbf{I}$ the identity matrix.

One important aspect is that the elements of $\mathbf{x}$ (e.g. linear velocity and angular velocity of the WMR) may be of different dimensions (e.g. m/s and s^{-1}). Consequently, the associated singular values have different units (e.g. m^{-1} and dimensionless) and it is impossible to order them[12]. In order to overcome this problem, a *characteristic length* D has to be introduced[13] (e.g. the angular velocity would be multiplied by D and its associated column divided by D). This parameter has been traditionally optimized in robot manipulators in order to give the best accuracy (isotropy), known as *natural length*.[14] This option will be considered in Section 3. A practical interpretation of the characteristic length for linear and angular velocities is shown by Stocco *et al.*[15–16] as the relative capability to translate and rotate with equal wheel velocities values. Therefore, they suggest that the characteristic length should be chosen to better satisfy the demands of motion and should not be a free design parameter. If so, simply one extra WMR parameter should be properly designed in order to achieve isotropy, as pointed out in subsections 3.3 and 3.4.

For our purpose, the input vectors $\mathbf{y}$ are the assigned velocities $\dot{\mathbf{q}}_{\mathrm{a}}$, so only m $(n = m)$ scalar equations from (9) can be considered in the isotropy analysis. Then, the isotropy conditions will be established for no error amplification between the input data vector $\dot{\mathbf{q}}_{\mathrm{a}}$ and the output variable vector $\dot{\mathbf{q}}_{\mathrm{na\_s}}$, both with m scalar elements, and vice versa. The procedure from (8) is:

$$\begin{pmatrix} \dot{\mathbf{q}}_{\mathrm{na\_ns}} \\ \dot{\mathbf{q}}_{\mathrm{na\_s}} \\ \dot{\mathbf{q}}_{\mathrm{a}} \end{pmatrix} = \begin{pmatrix} \mathbf{B}_{\mathrm{na\_ns}} \\ \mathbf{B}_{\mathrm{na\_s}} \\ \mathbf{B}_{\mathrm{a}} \end{pmatrix} \boldsymbol{\eta} \to \begin{cases} \dot{\mathbf{q}}_{\mathrm{na\_s}} = \left(\mathbf{B}_{\mathrm{na\_s}}\mathbf{B}_{\mathrm{a}}^{-1}\right) \dot{\mathbf{q}}_{\mathrm{a}} \\ \left(\mathbf{B}_{\mathrm{a}}\mathbf{B}_{\mathrm{na\_s}}^{-1}\right) \dot{\mathbf{q}}_{\mathrm{na\_s}} = \dot{\mathbf{q}}_{\mathrm{a}}, \end{cases} \tag{15}$$

where $\dot{\mathbf{q}}_{\mathrm{na\_ns}}$ are the remaining velocities not considered for isotropy. Note that both $\mathbf{B}_{\mathrm{a}}$ and $\mathbf{B}_{\mathrm{na\_s}}$ must be in general non singular, i.e. not any $\dot{\mathbf{q}}_{\mathrm{na\_s}}$ and $\dot{\mathbf{q}}_{\mathrm{a}}$vectors are possible for an isotropy analysis, which depends upon $\mathbf{H} = \mathbf{B}_{\mathrm{a}}\,(\mathbf{B}_{\mathrm{an\_s}})^{-1}$.

It is derived the following *criterion*: *isotropy* (no relative error amplification) *has to be achieved*. In particular, when the WMR has no *orientable* or *castor* wheels, this becomes *design criterion*, since the conditions for isotropy are permanent. In contrast, if there are *orientable* or *castor* wheels, the conditions are achieved for specific configurations, *isotropic configurations*, and the criterion is a *planning* or *control criterion*. In this case, an over-actuated WMR would be useful, since it allows change from one kinematic model to another, thus benefiting from the isotropy of the second one. A possible *design criterion* for the second case could even be to compute the WMR parameter values (e.g. wheel radius, distances. . .) in order to minimize the average of the condition number across the configuration space, what leads to the global isotropy concept. The generic criterion here indicated is perfectly complemented by the criterion: *singularity has to be avoided*.[4]

3. Kinematic Models and Isotropy for the 5 Types of Wheeled Mobile Robots

3.1. Introduction

Campion *et al.*[1] showed that WMRs could be classified into five generic types and they obtained their forward

https://doi.org/10.1017/S0263574708004165 Published online by Cambridge University Press

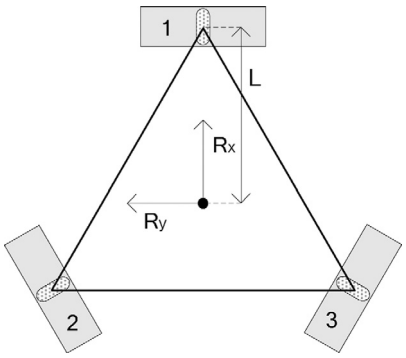

Fig. 3. Omnidirectional (Type I) and isotropic WMR with *Swedish* wheels.

kinematic models for the three wheel case. Nevertheless, these kinematic models have input variables with no physical meaning while wheel velocities do not appear. This is due to the fact that only a few equations, i.e. the first element of (2), were used. Therefore, in order to extend that work, the five generic WMRs with three wheels are modeled in this section including all the WMR velocities and wheel velocities (except the roller rotation velocity $\dot{\varphi}_{ri}$ of a *Swedish* wheel, since that variable is usually not accessible in practice, what implies that the first element of (3) is omitted). Accordingly, the procedures described in subsections 2.2 and 2.3 are applied for modeling and isotropy analysis. The fact of considering WMRs with three wheels is for stability reasons, and implies no loss of generality. In the next subsections, the same wheels parameters r_i, r_{ri}, d_i, δ_i, and γ_i will be assumed (when applicable). The widely used roller orientation of 90° for *Swedish* wheels ($\gamma = 90°$) and the usual zero value for *castor* wheel orientation with respect to the steering link ($\delta = 0$) will also be considered. Furthermore, in the subsequent developments a compact trigonometric notation will be used: $\cos(x) \equiv \mathrm{c}x$, $\sin(x) \equiv \mathrm{s}x$.

3.2. *Type I: Omnidirectional WMR*

This type of WMR has full mobility ($m = 3$) and is constructed with no *fixed* or *orientable* wheels, i.e. with either *Swedish* or *castor* wheels. This study considers two options: three *Swedish* wheels and three *castor* wheels.

3.2.1. Omnidirectional WMR with three Swedish wheels. With the procedure shown in subsection 2.2 the kinematic solution (6) is obtained:

$$\begin{pmatrix} \dot{\mathbf{p}} \\ \dot{\boldsymbol{\varphi}} \end{pmatrix} = \begin{pmatrix} -\mathrm{s}\gamma \mathrm{r}\mathbf{I} \\ \mathbf{A}_\mathrm{p} \end{pmatrix} \boldsymbol{\eta} \quad \dot{\boldsymbol{\varphi}} = \begin{pmatrix} \dot{\varphi}_1 \\ \dot{\varphi}_2 \\ \dot{\varphi}_3 \end{pmatrix}$$

$$\mathbf{A}_\mathrm{p} = \begin{pmatrix} \mathrm{c}(\beta_1+\gamma) & \mathrm{s}(\beta_1+\gamma) & \mathrm{l}_1\mathrm{s}(\beta_1+\gamma-\alpha_1) \\ \mathrm{c}(\beta_2+\gamma) & \mathrm{s}(\beta_2+\gamma) & \mathrm{l}_2\mathrm{s}(\beta_2+\gamma-\alpha_2) \\ \mathrm{c}(\beta_3+\gamma) & \mathrm{s}(\beta_3+\gamma) & \mathrm{l}_3\mathrm{s}(\beta_3+\gamma-\alpha_3) \end{pmatrix}. \tag{16}$$

The forward and inverse kinematic models result:

$$\dot{\mathbf{p}} = -\mathrm{r}\,\mathrm{s}\gamma \mathbf{A}_\mathrm{p}^{-1}\dot{\boldsymbol{\varphi}} \qquad \dot{\boldsymbol{\varphi}} = -(\mathrm{r}\,\mathrm{s}\gamma)^{-1}\mathbf{A}_\mathrm{p}\,\dot{\mathbf{p}}. \tag{17}$$

The isotropy for both forward and inverse kinematics in (17) depends upon matrix $\mathbf{A}_\mathrm{p}$. As already mentioned in subsection 2.3, the complete isotropy analysis can be found in Saha *et al.*,[5] so it is not going to be duplicated here. The result is that the centers of the three wheels represent the vertices of a regular (*equilateral*) triangle and the plane of each wheel is perpendicular to the line joining the *centroid* of the triangle and the wheel center. If frame R is located on this centroid and its X-axis crosses the first wheel center (Fig. 3), the parameters are $\{\alpha_1 = 0, \alpha_2 = 120°, \alpha_3 = 240°, \beta_i = \alpha_i, \mathrm{l}_i = \mathrm{L}\}$, and (17) result in:

$$\dot{\mathbf{p}} = \frac{\mathrm{r}}{3}\begin{pmatrix} 0 & \sqrt{3} & -\sqrt{3} \\ -2 & 1 & 1 \\ -1/\mathrm{L} & -1/\mathrm{L} & -1/\mathrm{L} \end{pmatrix} \dot{\boldsymbol{\varphi}}$$

$$\dot{\boldsymbol{\varphi}} = \frac{1}{\mathrm{r}}\begin{pmatrix} 0 & -1 & -\mathrm{L} \\ \sqrt{3}/2 & 0.5 & -\mathrm{L} \\ -\sqrt{3}/2 & 0.5 & -\mathrm{L} \end{pmatrix} \dot{\mathbf{p}}. \tag{18}$$

3.2.2. Omnidirectional WMR with three castor wheels. With the procedure shown in subsection 2.2 the kinematic solution (6) is obtained:

$$\begin{pmatrix} \dot{\mathbf{p}} \\ \dot{\boldsymbol{\beta}} \\ \dot{\boldsymbol{\varphi}} \end{pmatrix} = \begin{pmatrix} \mathbf{I} \\ (1/\mathrm{d})\mathbf{A}_{\mathrm{p}1} \\ -(1/\mathrm{r})\mathbf{A}_{\mathrm{p}2} \end{pmatrix} \boldsymbol{\eta}$$

$$\dot{\boldsymbol{\beta}} = \begin{pmatrix} \dot{\beta}_1 \\ \dot{\beta}_2 \\ \dot{\beta}_3 \end{pmatrix} \mathbf{A}_{\mathrm{p}1} = \begin{pmatrix} \mathrm{c}\beta_1 & \mathrm{s}\beta_1 & \mathrm{l}_1\mathrm{s}(\beta_1-\alpha_1)-\mathrm{d} \\ \mathrm{c}\beta_2 & \mathrm{s}\beta_2 & \mathrm{l}_2\mathrm{s}(\beta_2-\alpha_2)-\mathrm{d} \\ \mathrm{c}\beta_3 & \mathrm{s}\beta_3 & \mathrm{l}_3\mathrm{s}(\beta_3-\alpha_3)-\mathrm{d} \end{pmatrix}$$

$$\dot{\boldsymbol{\varphi}} = \begin{pmatrix} \dot{\varphi}_1 \\ \dot{\varphi}_2 \\ \dot{\varphi}_3 \end{pmatrix} \mathbf{A}_{\mathrm{p}2} = \begin{pmatrix} -\mathrm{s}\beta_1 & \mathrm{c}\beta_1 & \mathrm{l}_1\mathrm{c}(\beta_1-\alpha_1) \\ -\mathrm{s}\beta_2 & \mathrm{c}\beta_2 & \mathrm{l}_2\mathrm{c}(\beta_2-\alpha_2) \\ -\mathrm{s}\beta_3 & \mathrm{c}\beta_3 & \mathrm{l}_3\mathrm{c}(\beta_3-\alpha_3) \end{pmatrix}. \tag{19}$$

The forward kinematic models with $\dot{\boldsymbol{\beta}}$ or $\dot{\boldsymbol{\varphi}}$ as assigned velocities and the inverse model are:

$$\begin{pmatrix} \dot{\mathbf{p}} \\ \dot{\boldsymbol{\varphi}} \end{pmatrix} = \mathrm{d}\begin{pmatrix} \mathbf{A}_{\mathrm{p}1}^{-1} \\ -(1/\mathrm{r})\,\mathbf{A}_{\mathrm{p}2}\,\mathbf{A}_{\mathrm{p}1}^{-1} \end{pmatrix} \dot{\boldsymbol{\beta}}$$

$$\begin{pmatrix} \dot{\mathbf{p}} \\ \dot{\boldsymbol{\beta}} \end{pmatrix} = -\mathrm{r}\begin{pmatrix} \mathbf{A}_{\mathrm{p}2}^{-1} \\ (1/\mathrm{d})\mathbf{A}_{\mathrm{p}1}\mathbf{A}_{\mathrm{p}2}^{-1} \end{pmatrix} \dot{\boldsymbol{\varphi}}$$

$$\begin{pmatrix} \dot{\boldsymbol{\beta}} \\ \dot{\boldsymbol{\varphi}} \end{pmatrix} = \begin{pmatrix} (1/\mathrm{d})\mathbf{A}_{\mathrm{p}1} \\ -(1/\mathrm{r})\mathbf{A}_{\mathrm{p}2} \end{pmatrix} \dot{\mathbf{p}}. \tag{20}$$

Low and Leow[6] showed that the isotropy of the forward and inverse kinematics is achieved if $\mathrm{d} = \mathrm{r}$ and the steering axles of the three wheels are on the vertices of an equilateral triangle. Nevertheless, that isotropy result is only valid as long as the steering link distance d is negligible with respect to the distance between the triangle centroid and

https://doi.org/10.1017/S0263574708004165 Published online by Cambridge University Press

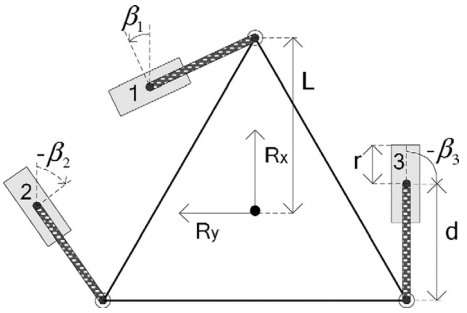

Fig. 4. Omnidirectional and quasi-isotropic WMR with *castor* wheels.

the steering axle. Otherwise, the isotropy conditions depend on the variable steering angles. In fact, a complete isotropy analysis (for $\dot{\mathbf{q}}_{\text{na\_s}} = \dot{\mathbf{p}}$) can be found in Kim *et al.*,[7] were the isotropic configurations (i.e. the values of $\boldsymbol{\beta}$) are characterized in the forward kinematic model depending on the set of assigned wheel velocities. Moreover, these authors developed[8–9] a global isotropy optimization through the characteristic length. They defined the global isotropy, for a set of assigned velocities, as the average of the inverse of the condition number (local isotropy) across the configuration space given by $\boldsymbol{\beta}$. Moreover, both group of researchers occasionally considered more than three assigned velocities (e.g. actuated joints), although this would be outside the no-slip framework of (6), since only three velocities can be assigned independently.

With the isotropy conditions of Low and Leow[6] and locating frame R on the triangle centroid, with its X-axis crossing the steering axle of the first wheel (see Fig. 4), the parameters result in: $\{\alpha_1 = 0, \alpha_2 = 120^\circ, \alpha_3 = 240^\circ, \mathrm{l}_i = \mathrm{L}, \mathrm{r} = \mathrm{d}\}$(the substitution in (20) is omitted since the models are not simplified).

3.3. Type II: Differential-drive WMR

This WMR has one independent *fixed* wheel and other possibly omnidirectional wheels, thus the mobility is 2. This study considers two dependent *fixed* wheels (differential-drive wheel mechanism) and another omnidirectional wheel, either *Swedish* or *castor*. Taken into account where has been located frame R (see Fig. 5 (a) and Fig. 5 (d)) the parameters result $\{\beta_1 = \beta_2 = \alpha_1 = 0,\ \alpha_2 = \pi, \mathrm{l}_1 = \mathrm{l}_2 = \mathrm{L}\}$.

3.3.1. Differential-drive WMR with a Swedish wheel. Exceptionally, for this WMR (Fig. 5 (a)) it will not be assume the same radius for the 3 wheels. With the procedure shown in subsection 2.2 the kinematic solution (6) for this WMR is:

$$\begin{pmatrix} \dot{\mathbf{p}} \\ \dot{\varphi}_1 \\ \dot{\varphi}_2 \\ \dot{\varphi}_3 \end{pmatrix} = \begin{pmatrix} 0 & 0 \\ -\mathrm{L} & -\mathrm{l} \\ -1 & 1 \\ 2\mathrm{L}/\mathrm{r}_1 & 0 \\ 0 & 2\mathrm{L}/\mathrm{r}_2 \\ (\mathrm{L}c\beta_3 + \mathrm{l}_3 c(\beta_3 - \alpha_3))/\mathrm{r}_3 & (\mathrm{L}c\beta_3 - \mathrm{l}_3 c(\beta_3 - \alpha_3))/\mathrm{r}_3 \end{pmatrix} \boldsymbol{\eta}. \tag{21}$$

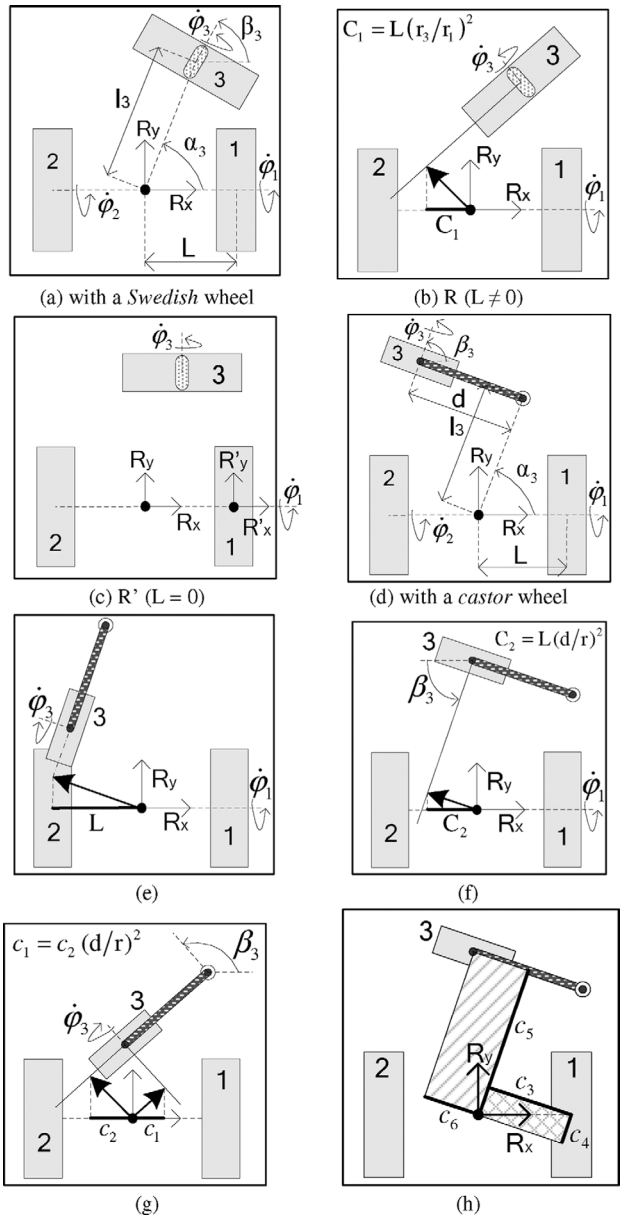

Fig. 5. Differential-drive WMR with a *Swedish* or *castor* wheel and its isotropic configurations.

The forward and inverse kinematic models could be obtained straightforward from (21) applying (9) for any pair of assigned velocities not including v_x. In particular, for the isotropy analysis it will be considered the relationships between the non-zero WMR velocities and wheel velocities:

$$\begin{pmatrix} -1/\mathrm{r}_1 & -\mathrm{L}/\mathrm{r}_1 \\ -1/\mathrm{r}_2 & \mathrm{L}/\mathrm{r}_2 \end{pmatrix} \begin{pmatrix} v_y \\ \omega \end{pmatrix} = \begin{pmatrix} \dot{\varphi}_1 \\ \dot{\varphi}_2 \end{pmatrix} \tag{22}$$

$$\begin{pmatrix} -1/\mathrm{r}_1 & -\mathrm{L}/\mathrm{r}_1 \\ -c\beta_3/\mathrm{r}_3 & -\mathrm{l}_3 c\,(\beta_3 - \alpha_3)/\mathrm{r}_3 \end{pmatrix} \begin{pmatrix} v_y \\ \omega \end{pmatrix} = \begin{pmatrix} \dot{\varphi}_1 \\ \dot{\varphi}_3 \end{pmatrix}. \tag{23}$$

As mentioned in subsection 2.3, it is necessary to introduce in $\{(22), (23)\}$ the characteristic lengths $\{\mathrm{D}_1, \mathrm{D}_2\}$ as follows:

$$\begin{pmatrix} -1/\mathrm{r}_1 & -\mathrm{L}/(\mathrm{r}_1\mathrm{D}_1) \\ -1/\mathrm{r}_2 & \mathrm{L}/(\mathrm{r}_2\mathrm{D}_1) \end{pmatrix} \begin{pmatrix} v_y \\ \mathrm{D}_1\omega \end{pmatrix} = \begin{pmatrix} \dot{\varphi}_1 \\ \dot{\varphi}_2 \end{pmatrix} \tag{24}$$

https://doi.org/10.1017/S0263574708004165 Published online by Cambridge University Press

$$\begin{pmatrix} -1/r_1 & -L/(r_1 D_2) \\ -c\beta_3/r_3 & -l_3 \cdot c\,(\beta_3-\alpha_3)/(r_3 D_2) \end{pmatrix} \begin{pmatrix} v_y \\ D_2\omega \end{pmatrix} = \begin{pmatrix} \dot\varphi_1 \\ \dot\varphi_3 \end{pmatrix}. \tag{25}$$

In order to establish the isotropy conditions, (14) is applied:

$$\begin{pmatrix} 1/r_1^2 + 1/r_2^2 & (L/D_1)\left(1/r_1^2 - 1/r_2^2\right) \\ (L/D_1)\left(1/r_1^2 - 1/r_2^2\right) & (L/D_1)^2\left(1/r_1^2 + 1/r_2^2\right) \end{pmatrix} = k_1 \mathbf{I} \tag{26}$$

$$\begin{pmatrix} \frac{1}{r_1^2} + \left(\frac{c\beta_3}{r_3}\right)^2 & \frac{1}{D_2 r_1^2} + \frac{l_3 c\beta_3 c\,(\beta_3-\alpha_3)}{r_3^2\, D_2} \\ \frac{L}{D_2 r_1^2} + \frac{l_3 c\beta_3 c\,(\beta_3-\alpha_3)}{r_3^2\, D_2} & \left(\frac{L^2}{D_2^2 r_1^2} + \left(\frac{l_3 c(\beta_3-\alpha_3)}{r_3 D_2}\right)^2\right) \end{pmatrix} = k_2 \mathbf{I}. \tag{27}$$

By virtue of (26), the isotropic relationship between the non-zero WMR velocities $(v_y, D_1\omega)$ and the rotation velocities of both *fixed* wheels $(\dot\varphi_1, \dot\varphi_2)$ is given by:

$$\{(v_y, D_1\omega) \leftrightarrow (\dot\varphi_1, \dot\varphi_2)\} \rightarrow r_1 = r_2 \quad \text{and} \quad D_1 = L\,. \tag{28}$$

In the same way, eq. (27) becomes:

$$\begin{Bmatrix} (v_y, D_2\omega) \\ \updownarrow \\ (\dot\varphi_1, \dot\varphi_3) \end{Bmatrix} \rightarrow \begin{cases} c\beta_3 l_3 c(\beta_3-\alpha_3) = -L(r_3/r_1)^2 \rightarrow \text{Fig. 5 (b)} \\ D_2 = \sqrt{\dfrac{(Lr_3)^2 + (l_3 c\,(\beta_3-\alpha_3)\, r_1)^2}{r_3^2 + (c\beta_3 r_1)^2}}. \end{cases} \tag{29}$$

In Fig. 5(b) it is geometrically represented the first condition of (29). If it is considered a frame R' (instead of R) located on the first *fixed* wheel, (29) is valid but with $L = 0$. In that case the isotropy condition is given by $\beta_3 = \pm 90^\circ$ (Fig. 5(c)), where the forward motion is provided by the rotation of the *fixed* wheel and the angular motion by the rotation of the *Swedish* wheel. Note that the solutions $\beta_3 - \alpha_3 = \pm 90^\circ$ and $l_3 = 0$ are not valid because a kinematic singularity arises[4].

3.3.2. Differential-drive WMR with a castor wheel. The kinematic solution of (6) for this WMR (Fig. 5 (d)) is:

$$\begin{pmatrix} \dot{\mathbf{p}} \\ \dot\varphi_1 \\ \dot\varphi_2 \\ \dot\varphi_3 \\ \dot\beta_3 \end{pmatrix} = \begin{pmatrix} 0 & 0 \\ -L & -L \\ -1 & 1 \\ 2L/r & 0 \\ 0 & 2L/r \\ \dfrac{(Lc\beta_3 + l_3 c\,(\beta_3-\alpha_3))}{r} & \dfrac{(Lc\beta_3 - l_3 c\,(\beta_3-\alpha_3))}{r} \\ -\dfrac{Ls\beta_3 + l_3 s\,(\beta_3-\alpha_3)}{d} + 1 & -\dfrac{Ls\beta_3 - l_3 s\,(\beta_3-\alpha_3)}{d} - 1 \end{pmatrix} \boldsymbol{\eta}. \tag{30}$$

As before, for this WMR any pair of velocities not including v_x can be assigned. Meanwhile, with the procedure shown in previous point 3.2.1, the isotropy conditions between each two pair of velocities result:

$$\{(v_y, D_3\omega) \leftrightarrow (\dot\varphi_1, \dot\varphi_2)\} \rightarrow \; D_3 = L \tag{31}$$

$$\{(v_y, D_4\omega) \leftrightarrow (\dot\varphi_1, \dot\varphi_3)\} \rightarrow \begin{cases} c\beta_3\, l_3\, c(\beta_3-\alpha_3) = -L \rightarrow \text{Fig. 5 (e)} \\ D_4 = \sqrt{(L^2 + l_3^2 c^2(\beta_3-\alpha_3))/(1+c^2\beta_3)} \end{cases} \tag{32}$$

$$\begin{Bmatrix} (v_y, D_5\omega) \\ \updownarrow \\ (\dot\varphi_1, \dot\beta_3) \end{Bmatrix} \rightarrow \begin{cases} s\beta_3\left(l_3\, s\,(\beta_3-\alpha_3) - d\right) = -(d/r)^2 L \rightarrow \text{Fig. 5 (f)} \\ D_5 = \sqrt{(L^2 d^2 + r^2(l_3\, s\,(\beta_3-\alpha_3) - d)^2)/(d^2 + r^2\, s^2\beta_3)} \end{cases} \tag{33}$$

$$\begin{Bmatrix} (v_y, D_6\omega) \\ \updownarrow \\ (\dot\varphi_3, \dot\beta_3) \end{Bmatrix} \rightarrow \begin{cases} (d/r)^2\, l_3 c\beta_3 c\,(\beta_3-\alpha_3) = (d/r)^2\, c_2 = \\ = -s\beta_3\left(l_3 s\,(\beta_3-\alpha_3) - d\right) = c_1 \rightarrow \text{Fig. 5 (g)} \\ D_6 = \sqrt{\dfrac{d^2 l_3^2\, c^2\,(\beta_3-\alpha_3) + r^2(l_3\, s\,(\beta_3-\alpha_3) - d)^2}{(d\, c\beta_3)^2 + (r\, s\beta_3)^2}} \end{cases} \tag{34}$$

$$\{(\dot\varphi_1, \dot\varphi_2) \leftrightarrow (\dot\varphi_3, \dot\beta_3)\} \rightarrow \begin{cases} c_5\; c_6 = c_3\; c_4 \\ c_3^2 + c_6^2 = (d^2/r^2)\left(c_4^2 + c_5^2\right) \end{cases}$$
$$\text{where (Fig. 5 (h))} \; c_3 = Ls\beta_3 \qquad c_4 = Lc\beta_3 \tag{35}$$
$$c_5 = l_3 c(\beta_3-\alpha_3) \; c_6 = d - l_3 s(\beta_3-\alpha_3).$$

Note that, in order to achieve the isotropy conditions of (35) for one configuration β_3, one parameter (i.e. α_3, l_3, d, L, ...) has to be designed properly. The same is applicable to (32)–(34) if the characteristic lengths are not free design parameters.

3.4. Type III: WMR with one orientable wheel

This WMR has one independent *orientable* wheel and other other possibly omnidirectional wheels ($m = 2$). This study considers one *orientable* wheel and two omnidirectional wheels of the same type: *Swedish* (Fig. 6(a)) or *castor* (Fig. 6(d)). For this WMR, the origin of frame R has been located at the center of the orientable wheel (Fig. 6), so $l_1 = 0$. The kinematic solution for each WMR is (36) and (39). For both WMRs, any pair of velocities can be considered assigned except $(v_x \quad v_y)^T$. Note that, Eqs. (36) and (39) are inverse kinematic models, where the assigned velocities are the forward motion of the WMR in the direction of the orientable wheel plane and the WMR angular motion. With the procedure shown in point 3.2.1, the isotropy conditions between a pair of WMR velocities and a pair of wheel velocities result {(37), (38)} and {(40)–(45)}. Note that, the permanent solutions $\{\beta_2 - \alpha_2 = \pm 90^\circ\}$ for (37) and $\{\beta_2 - \alpha_2 = \beta_3 - \alpha_3 = \pm 90^\circ\}$ for (38) are not valid because a kinematic singularity arises.[4] In the same way, the solution $\beta_1 = \beta_2 = \beta_3$, that fulfills simultaneously (37) and (38), is not valid because a kinematic singularity arises[4]. As before, if the characteristic lengths of {(37), (38), (40)–(45)} are not free

https://doi.org/10.1017/S0263574708004165 Published online by Cambridge University Press

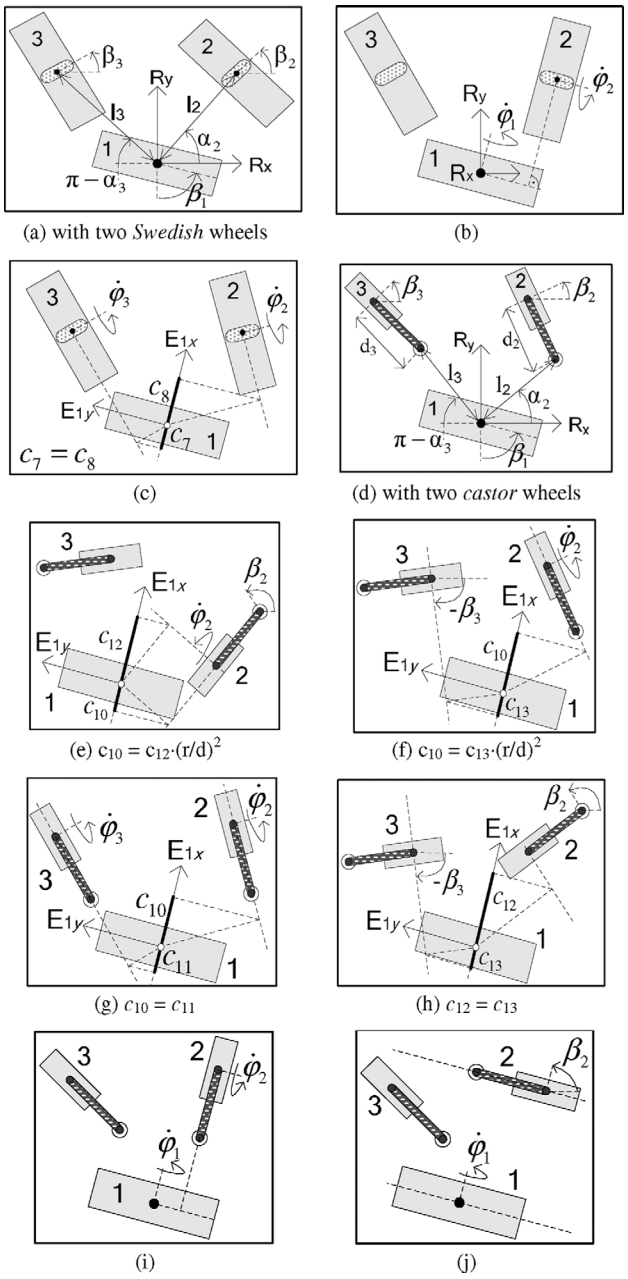

Fig. 6. WMR with one *orientable* wheel and two *Swedish*/*castor* wheels.

design parameters, one extra parameter (i.e. α_2, α_3, $l_2 \ldots$) has to be designed properly to achieve the isotropy conditions.

$$\begin{pmatrix} \dot{\mathbf{p}} \\ \dot{\varphi}_1 \\ \dot{\varphi}_2 \\ \dot{\varphi}_3 \end{pmatrix} = \begin{pmatrix} \mathrm{s}\beta_1 & 0 \\ -\mathrm{c}\beta_1 & 0 \\ 0 & 1 \\ 1/\mathrm{r} & 0 \\ \mathrm{c}(\beta_1-\beta_2)/\mathrm{r} & -\mathrm{l}_2\mathrm{c}(\beta_2-\alpha_2)/\mathrm{r} \\ \mathrm{c}(\beta_1-\beta_3)/\mathrm{r} & -\mathrm{l}_3\mathrm{c}(\beta_3-\alpha_3)/\mathrm{r} \end{pmatrix} \boldsymbol{\eta} \tag{36}$$

$$\left\{ \begin{pmatrix} (v_x, \mathrm{D}_7\omega) \\ (v_y, \mathrm{D}_7\omega) \\ (\eta_1, \mathrm{D}_7\eta_2) \end{pmatrix} \leftrightarrow (\dot{\varphi}_1, \dot{\varphi}_2) \right\}$$

$$\rightarrow \begin{cases} \mathrm{c}(\beta_1-\beta_2)\,\mathrm{c}(\beta_2-\alpha_2) = 0 \rightarrow \text{Fig. 6 (b)} \\ \mathrm{D}_7 = \mathrm{l}_2\mathrm{c}(\beta_2-\alpha_2)/\sqrt{1+\mathrm{c}^2(\beta_1-\beta_2)} \end{cases} \tag{37}$$

$$\left\{ \begin{pmatrix} (v_x, \mathrm{D}_8\omega) \\ (v_y, \mathrm{D}_8\omega) \\ (\eta_1, \mathrm{D}_8\eta_2) \end{pmatrix} \leftrightarrow (\dot{\varphi}_2, \dot{\varphi}_3) \right\}$$

$$\rightarrow \begin{cases} \mathrm{l}_3\mathrm{c}(\beta_1-\beta_3)\,\mathrm{c}(\beta_3-\alpha_3) = \\ = -\mathrm{l}_2\mathrm{c}(\beta_1-\beta_2)\,\mathrm{c}(\beta_2-\alpha_2) \rightarrow \text{Fig. 6 (c)} \\ \mathrm{D}_8 = \dfrac{\sqrt{\mathrm{l}_2^2\mathrm{c}^2(\beta_2-\alpha_2)+\mathrm{l}_3^2\mathrm{c}^2(\beta_3-\alpha_3)}}{\sqrt{\mathrm{c}^2(\beta_1-\beta_2)+\mathrm{c}^2(\beta_1-\beta_3)}} \end{cases} \tag{38}$$

$$\begin{pmatrix} \dot{\mathbf{p}} \\ \dot{\varphi}_1 \\ \dot{\varphi}_2 \\ \dot{\varphi}_3 \\ \dot{\beta}_2 \\ \dot{\beta}_3 \end{pmatrix} = \begin{pmatrix} \mathrm{s}\beta_1 & 0 \\ -\mathrm{c}\beta_1 & 0 \\ 0 & 1 \\ 1/\mathrm{r} & 0 \\ \mathrm{c}\beta_{12}/\mathrm{r} & -\mathrm{l}_2\mathrm{c}\beta_{22}/\mathrm{r} \\ \mathrm{c}\beta_{13}/\mathrm{r} & -\mathrm{l}_3\mathrm{c}\beta_{33}/\mathrm{r} \\ \mathrm{s}\beta_{12}/\mathrm{d} & \mathrm{l}_2\mathrm{s}\beta_{22}/\mathrm{d}-1 \\ \mathrm{s}\beta_{13}/\mathrm{d} & \mathrm{l}_3\mathrm{s}\beta_{33}/\mathrm{d}-1 \end{pmatrix} \boldsymbol{\eta} \quad \text{where} \begin{cases} \beta_{12} = \beta_1 - \beta_2 \\ \beta_{13} = \beta_1 - \beta_3 \\ \beta_{22} = \beta_2 - \alpha_2 \\ \beta_{33} = \beta_3 - \alpha_3 \end{cases} \tag{39}$$

$$\left\{ \begin{pmatrix} (v_x, \mathrm{D}_9\omega) \\ (v_y, \mathrm{D}_9\omega) \\ (\eta_1, \mathrm{D}_9\eta_2) \end{pmatrix} \leftrightarrow (\dot{\varphi}_1, \dot{\varphi}_2) \right\} \rightarrow \begin{cases} \mathrm{c}\beta_{12}\mathrm{c}\beta_{22} = 0 \rightarrow \text{Fig. 6 (i)} \\ \mathrm{D}_7 = \mathrm{l}_2\mathrm{c}\beta_{22}/\sqrt{1+\mathrm{c}^2\beta_{12}} \end{cases} \tag{40}$$

$$\left\{ \begin{pmatrix} (v_x, \mathrm{D}_{10}\omega) \\ (v_y, \mathrm{D}_{10}\omega) \\ (\eta_1, \mathrm{D}_{10}\eta_2) \end{pmatrix} \leftrightarrow (\dot{\varphi}_1, \dot{\beta}_2) \right\}$$

$$\rightarrow \begin{cases} \mathrm{s}\beta_{12}(\mathrm{d}-\mathrm{l}_2\mathrm{s}\beta_{22}) = 0 \rightarrow \text{Fig. 6 (j)} \\ \mathrm{D}_{10} = \dfrac{\mathrm{l}_2\mathrm{s}\beta_{22}-\mathrm{d}}{\sqrt{\mathrm{d}^2/\mathrm{r}^2+\mathrm{s}^2\beta_{12}}} \end{cases} \tag{41}$$

$$\left\{ \begin{pmatrix} (v_x, \mathrm{D}_{11}\omega) \\ (v_y, \mathrm{D}_{11}\omega) \\ (\eta_1, \mathrm{D}_{11}\eta_2) \end{pmatrix} \leftrightarrow (\dot{\varphi}_2, \dot{\varphi}_3) \right\}$$

$$\rightarrow \begin{cases} \mathrm{l}_2\mathrm{c}\beta_{22}\mathrm{c}\beta_{12} = -\mathrm{l}_3\mathrm{c}\beta_{33}\mathrm{c}\beta_{13} \rightarrow \text{Fig. 6 (g)} \\ \mathrm{D}_8 = \dfrac{\sqrt{\mathrm{l}_2^2\mathrm{c}^2\beta_{22}+\mathrm{l}_3^2\mathrm{c}^2\beta_{33}}}{\sqrt{\mathrm{c}^2\beta_{12}+\mathrm{c}^2\beta_{13}}} \end{cases} \tag{42}$$

$$\left\{ \begin{pmatrix} (v_x, \mathrm{D}_{12}\omega) \\ (v_y, \mathrm{D}_{12}\omega) \\ (\eta_1, \mathrm{D}_{12}\eta_2) \end{pmatrix} \leftrightarrow (\dot{\beta}_2, \dot{\beta}_3) \right\}$$

$$\rightarrow \begin{cases} \mathrm{s}\beta_{12}(\mathrm{d}-\mathrm{l}_2\mathrm{s}\beta_{22}) = \\ \quad -\mathrm{s}\beta_{13}(\mathrm{d}-\mathrm{l}_3\mathrm{s}\beta_{33}) \rightarrow \text{Fig. 6 (h)} \\ \mathrm{D}_{12} = \dfrac{\sqrt{(\mathrm{l}_2\mathrm{s}\beta_{22}-\mathrm{d})^2+(\mathrm{l}_3\mathrm{s}\beta_{33}-\mathrm{d})^2}}{\sqrt{\mathrm{s}^2\beta_{12}+\mathrm{s}^2\beta_{13}}} \end{cases} \tag{43}$$

https://doi.org/10.1017/S0263574708004165 Published online by Cambridge University Press

$$\left\{\begin{Bmatrix}(v_x,\mathrm{D}_{13}\omega)\\(v_y,\mathrm{D}_{13}\omega)\\(\eta_1,\mathrm{D}_{13}\eta_2)\end{Bmatrix}\leftrightarrow(\dot\varphi_2,\dot\beta_2)\right\}$$

$$\rightarrow\begin{cases}(\mathrm{r/d})^2\,\mathrm{s}\beta_{12}\,(\mathrm{d}-\mathrm{l}_2\mathrm{s}\beta_{22})=\\ \quad-\mathrm{l}_2\mathrm{c}\beta_{22}\mathrm{c}\beta_{12}\rightarrow\text{Fig. 6 (e)}\\ \mathrm{D}_{13}=\dfrac{\sqrt{\mathrm{d}^2\mathrm{l}_2^2\mathrm{c}^2\beta_{22}+\mathrm{r}^2\,(\mathrm{l}_2\mathrm{s}\beta_{22}-\mathrm{d})^2}}{\sqrt{\mathrm{d}^2\mathrm{c}^2\beta_{12}+\mathrm{r}^2\mathrm{s}^2\beta_{12}}}\end{cases}\tag{44}$$

$$\left\{\begin{Bmatrix}(v_x,\mathrm{D}_{14}\omega)\\(v_y,\mathrm{D}_{14}\omega)\\(\eta_1,\mathrm{D}_{14}\eta_2)\end{Bmatrix}\leftrightarrow(\dot\varphi_2,\dot\beta_3)\right\}$$

$$\rightarrow\begin{cases}(\mathrm{r/d})^2\,\mathrm{s}\beta_{13}\,(\mathrm{d}-\mathrm{l}_3\mathrm{s}\beta_{33})=\\ \quad-\mathrm{l}_2\mathrm{c}\beta_{22}\mathrm{c}\beta_{12}\rightarrow\text{Fig. 6 (f)}\\ \mathrm{D}_{14}=\dfrac{\sqrt{\mathrm{d}^2\mathrm{l}_2^2\mathrm{c}^2\beta_{22}+\mathrm{r}^2\,(\mathrm{l}_3\mathrm{s}\beta_{33}-\mathrm{d})^2}}{\sqrt{\mathrm{d}^2\mathrm{c}^2\beta_{12}+\mathrm{r}^2\mathrm{s}^2\beta_{13}}}\end{cases}\tag{45}$$

3.5. Type IV (tricycle and bicycle) and type V (two orientable wheels)

The type IV has one independent *orientable* wheel and another independent *fixed* wheel, meanwhile type V has two independent *orientable* wheels. Here, three options will be considered for type IV and two for type V (Fig. 7). Both type IV and type V have one degree of mobility (m=1) and therefore it makes no sense to apply isotropy since only one velocity is assigned and so far any relationship is scalar. It can bee seen in Fig. 7 where has been located frame R for each WMR. The kinematic solutions for type IV are {(46) (tricycle), (47) (bicycle with a *Swedish* wheel), (48) (bicycle with a *castor* wheel)} and for type V {(49) (type V with a *Swedish* wheel), (50) (type V with a *castor* wheel)}.

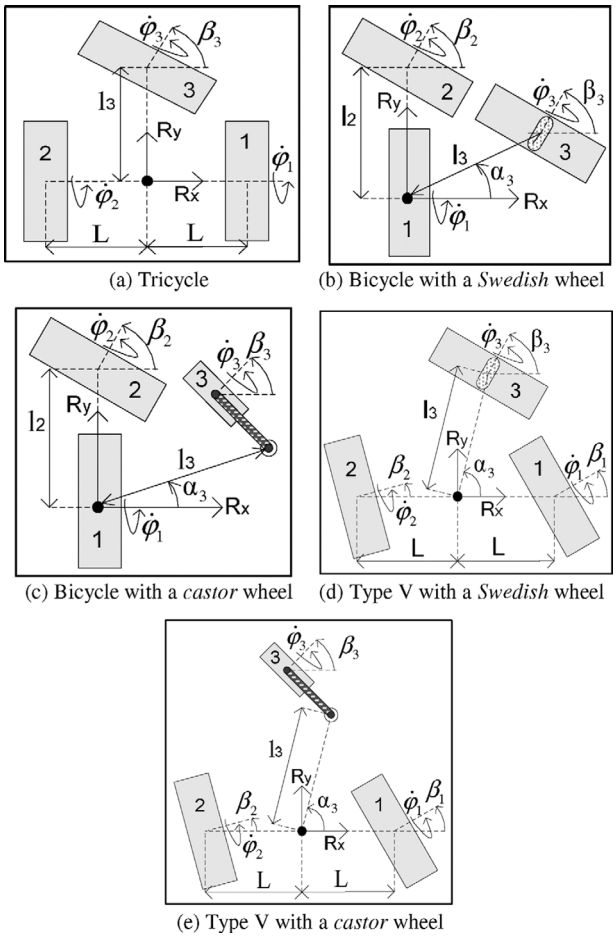

Fig. 7. Type IV and type V WMR.

$$\begin{pmatrix}\dot{\mathbf{p}}\\ \dot\varphi_1\\ \dot\varphi_2\\ \dot\varphi_3\end{pmatrix}=\begin{pmatrix}0\\ \mathrm{l}_3\mathrm{c}\beta_3\\ \mathrm{s}\beta_3\\ -\left(\mathrm{L}\mathrm{s}\beta_3+\mathrm{l}_3\mathrm{c}\beta_3\right)/\mathrm{r}\\ \left(\mathrm{L}\mathrm{s}\beta_3-\mathrm{l}_3\mathrm{c}\beta_3\right)/\mathrm{r}\\ -\mathrm{l}_3/\mathrm{r}\end{pmatrix}\eta\tag{46}$$

$$\begin{pmatrix}\dot{\mathbf{p}}\\ \dot\varphi_1\\ \dot\varphi_2\\ \dot\varphi_3\end{pmatrix}=\begin{pmatrix}0\\ \mathrm{l}_2\mathrm{c}\beta_2\\ \mathrm{s}\beta_2\\ -\mathrm{l}_2\mathrm{c}\beta_2/\mathrm{r}\\ -\mathrm{l}_2/\mathrm{r}\\ -(\mathrm{l}_3\mathrm{c}\,(\beta_3-\alpha_3)\,\mathrm{s}\beta_2+\mathrm{l}_2\mathrm{c}\beta_2\mathrm{c}\beta_3)/\mathrm{r}\end{pmatrix}\eta\tag{47}$$

$$\begin{pmatrix}\dot{\mathbf{p}}\\ \dot\varphi_1\\ \dot\varphi_2\\ \dot\varphi_3\\ \dot\beta_3\end{pmatrix}=\begin{pmatrix}0\\ \mathrm{l}_2\mathrm{c}\beta_2\\ \mathrm{s}\beta_2\\ -\mathrm{l}_2\mathrm{c}\beta_2/\mathrm{r}\\ -\mathrm{l}_2/\mathrm{r}\\ -(\mathrm{l}_3\mathrm{c}\,(\beta_3-\alpha_3)\,\mathrm{s}\beta_2+\mathrm{l}_2\mathrm{c}\beta_2\mathrm{c}\beta_3)/\mathrm{r}\\ ((\mathrm{l}_3\mathrm{s}\,(\beta_3-\alpha_3)-\mathrm{d})\mathrm{s}\beta_2+\mathrm{l}_2\mathrm{c}\beta_2\mathrm{s}\beta_3)/\mathrm{d}\end{pmatrix}\eta\tag{48}$$

$$\begin{pmatrix}\dot{\mathbf{p}}\\ \dot\varphi_1\\ \dot\varphi_2\\ \dot\varphi_3\end{pmatrix}=\begin{pmatrix}-2\,\mathrm{L}\,\mathrm{s}\beta_1\,\mathrm{s}\beta_2\\ \mathrm{L}\,\mathrm{s}\,(\beta_1+\beta_2)\\ \mathrm{s}\,(\beta_2-\beta_1)\\ -2\,\mathrm{L}\,\mathrm{s}\beta_2/\mathrm{r}\\ -2\,\mathrm{L}\,\mathrm{s}\beta_1/\mathrm{r}\\ -\begin{pmatrix}\mathrm{L}\,\mathrm{s}\,(\beta_1+\beta_2)\,\mathrm{c}\beta_3+2\,\mathrm{L}\,\mathrm{s}\beta_1\mathrm{s}\beta_2\mathrm{s}\beta_3\\ +\mathrm{l}_3\mathrm{s}\,(\beta_2-\beta_1)\,\mathrm{c}\,(\beta_3-\alpha_3)\end{pmatrix}\frac{1}{\mathrm{r}}\end{pmatrix}\eta\tag{49}$$

$$\begin{pmatrix}\dot{\mathbf{p}}\\ \dot\varphi_1\\ \dot\varphi_2\\ \dot\varphi_3\\ \dot\beta_3\end{pmatrix}=\begin{pmatrix}-2\,\mathrm{L}\,\mathrm{s}\beta_1\mathrm{s}\beta_2\\ \mathrm{L}\,\mathrm{s}\,(\beta_1+\beta_2)\\ \mathrm{s}\,(\beta_2-\beta_1)\\ -2\,\mathrm{L}\,\mathrm{s}\beta_2/\mathrm{r}\\ -2\,\mathrm{L}\,\mathrm{s}\beta_1/\mathrm{r}\\ -\begin{pmatrix}\mathrm{L}\,\mathrm{s}\,(\beta_1+\beta_2)\,\mathrm{c}\beta_3+2\,\mathrm{L}\,\mathrm{s}\beta_1\mathrm{s}\beta_2\mathrm{s}\beta_3\\ +\mathrm{l}_3\mathrm{s}\,(\beta_2-\beta_1)\,\mathrm{c}\,(\beta_3-\alpha_3)\end{pmatrix}\frac{1}{\mathrm{r}}\\ \begin{pmatrix}\mathrm{L}\,\mathrm{s}\,(\beta_1+\beta_2)\,\mathrm{s}\beta_3-2\,\mathrm{L}\,\mathrm{s}\beta_1\mathrm{s}\beta_2\mathrm{c}\beta_3\\ +\mathrm{s}\,(\beta_2-\beta_1)\,(\mathrm{l}_3\mathrm{s}\,(\beta_3-\alpha_3)-\mathrm{d})\end{pmatrix}\frac{1}{\mathrm{d}}\end{pmatrix}\eta\tag{50}$$

https://doi.org/10.1017/S0263574708004165 Published online by Cambridge University Press

4. Examples of Error Amplification

4.1. Differential-drive WMR

For the first example we consider type II WMR with the classical differentia-drive mechanism. In particular, relationship (24) will be analyzed using the characteristic length obtained in (28) and a generic radius for each wheel:

$$\begin{pmatrix} -1/r_1 & -1/r_1 \\ -1/r_2 & 1/r_2 \end{pmatrix} \begin{pmatrix} \nu_y \\ D_1\omega \end{pmatrix} = \begin{pmatrix} \dot{\varphi}_1 \\ \dot{\varphi}_2 \end{pmatrix} \rightarrow \mathbf{H}_1\mathbf{x}_1 = \mathbf{y}_1. \tag{51}$$

Assuming no uncertainty in the radii values, i.e. they are a priori known and constant, we have $\mathbf{F}_1 = 0$ and the maximum theoretical relative error amplification is given by the condition number of $\mathbf{H}_1$ (see (12)):

$$\left(\frac{\|\mathbf{x}_1(\in_1) - \mathbf{x}_1\|}{\|\mathbf{x}_1\|}\right) \Big/ \left(|\in_1| \frac{\|\mathbf{f}_1\|}{\|\mathbf{y}_1\|}\right) = \frac{\rho_{\mathbf{x}1}}{\rho_{\mathbf{y}1}} = \rho_{(\mathbf{x}_1\mathbf{y}_1)} \leq \kappa(\mathbf{H}_1) \tag{52}$$

where $\rho_{\mathbf{x}_1/\mathbf{y}_1}$ is the relative error amplification (hereinafter *error amplification*). For example, if it is considered the Euclidean norm it results:

$$\rho_{2(\mathbf{x}_1/\mathbf{y}_1)} \leq \kappa_2(\mathbf{H}_1) = \max(r_1, r_2)/\min(r_1, r_2). \tag{53}$$

It will be compared the error amplification and the theoretical maximum error amplification (i.e. $\kappa(\mathbf{H}_1)$) with respect to radius r_2. Note that isotropy is given by $r_2 = r_1$ (see (28)) and therefore X-axis will be *normalized* as $\log_{10}(r_2/r_1)$. For each value of r_2 it will be computed the error amplification for a *symmetric and uniform* probabilistic distribution for $\mathbf{y}_1$ and $\mathbf{f}_1$ (rotation velocities and rotation velocities error):

$$\mathbf{y}_1 = \begin{pmatrix} \dot{\varphi}_1 \\ \dot{\varphi}_2 \end{pmatrix} = \begin{pmatrix} -\dot{\varphi}_{\max} \cdots \dot{\varphi}_{\max} \\ -\dot{\varphi}_{\max} \cdots \dot{\varphi}_{\max} \end{pmatrix}$$
$$\mathbf{f}_1 = \begin{pmatrix} -\dot{\varphi}_{\text{error max}} \cdots \dot{\varphi}_{\text{error max}} \\ -\dot{\varphi}_{\text{error max}} \cdots \dot{\varphi}_{\text{error max}} \end{pmatrix}. \tag{54}$$

Furthermore, it will be computed the {average, maximum, minimum} of all the amplification values, e.g. 7808 values in Fig. 8. In particular, the *average* of the error amplification may be a good measure of the WMR real performance for a given radius r_2 when $\{\mathbf{y}_1, \mathbf{f}_1\}$ have not only one usual value. Nevertheless, it may be difficult to establish a priori the *usual* values of $\{\mathbf{y}_1, \mathbf{f}_1\}$ (e.g. (54)) to be used for computing the average.

In Figs. 8(a) and (b) it is shown the comparison between the error amplification and the theoretical maximum error amplification for the Euclidean norm. Note that, the graphs are symmetric with respect to the isotropy condition, and the curves of the error amplification are quite perfect although it has been used a finite set of points (7808). Note also that in Fig. 8(b) the maximum error amplification perfectly fits the theoretical maximum. It has been verified that the result is the same for Figs. 8(a) and 8(b) if the end points $\{\dot{\varphi}_{\max}, \dot{\varphi}_{\text{error max}}\}$ are changed. As an example, it will be detailed the error

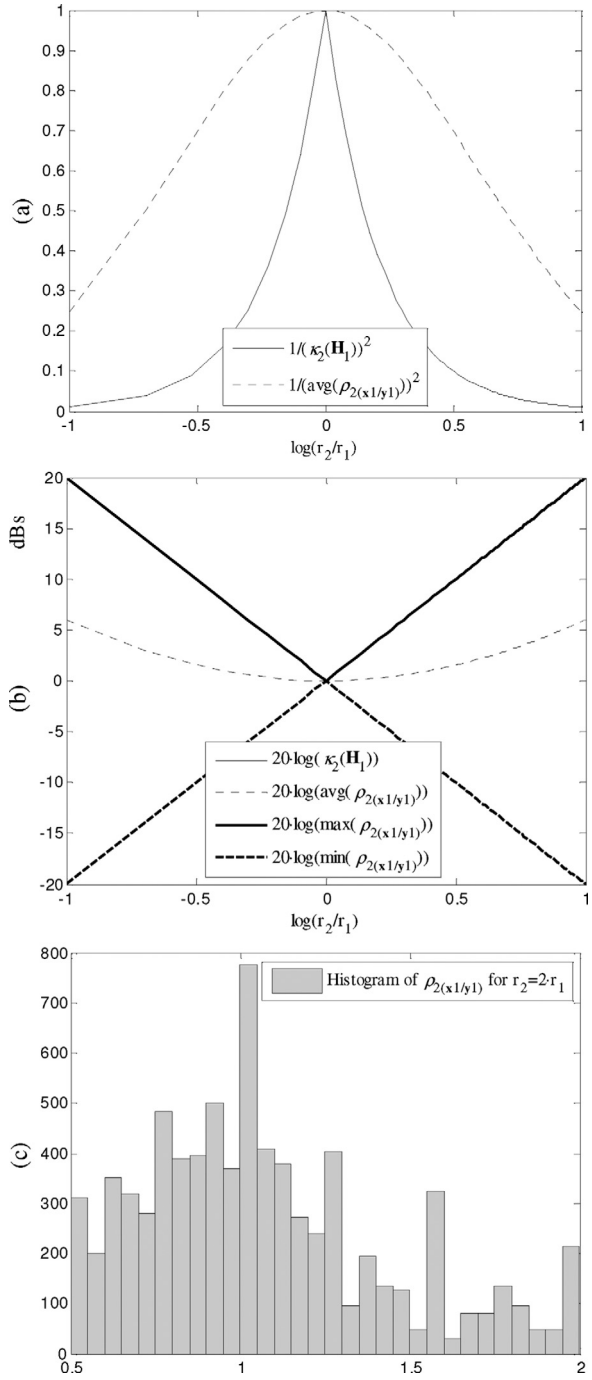

Fig. 8. Error amplification for the differential-drive WMR using the Euclidean norm, absolute error values for $\mathbf{f}_1$ and a symmetric and uniform probabilistic distribution for $\{\mathbf{y}_1, \mathbf{f}1\}$.

amplification for $r_2 = 2 \cdot r_1$:

$$\begin{aligned} &\text{avg}(\rho_{2(\mathbf{x}1/\mathbf{y}1)}) = 1.068764 \qquad \kappa_2(\mathbf{H}_1) = 2 \\ &\max(\rho_{2(\mathbf{x}1/\mathbf{y}1)}) = 2 \rightarrow \text{for}\{\mathbf{y}_1 = (-\dot{\varphi}_{\max}, \varepsilon)^{\mathrm{T}}, \\ &\quad \mathbf{f}_1 = (\varepsilon, -\dot{\varphi}_{\text{error max}})^{\mathrm{T}}\} \\ &\min(\rho_{2(\mathbf{x}1/\mathbf{y}1)}) = 0.5 \rightarrow \text{for } \{\mathbf{y}_1 = (\varepsilon, -\dot{\varphi}_{\max})^{\mathrm{T}}, \\ &\quad \mathbf{f}_1 = (-\dot{\varphi}_{\text{error max}}, \varepsilon)^{\mathrm{T}}\}, \end{aligned} \tag{55}$$

where ε is an arbitrary constant that tends to zero. In Fig. 8(c) it is represented the histogram of the error amplification for $r_2 = 2 \cdot r_1$, which has not a normal distribution.

https://doi.org/10.1017/S0263574708004165 Published online by Cambridge University Press

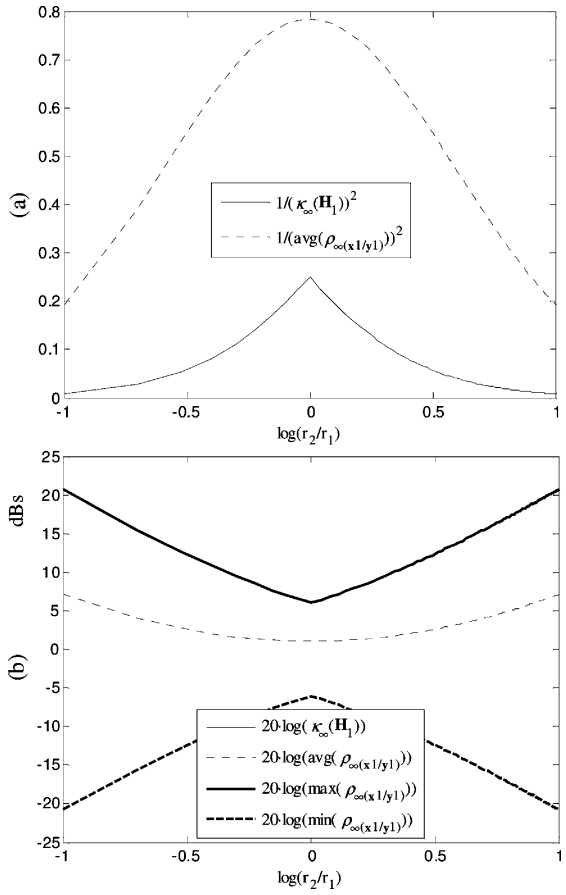

Fig. 9. Error amplification for the differential-drive WMR using the *infinity norm*.

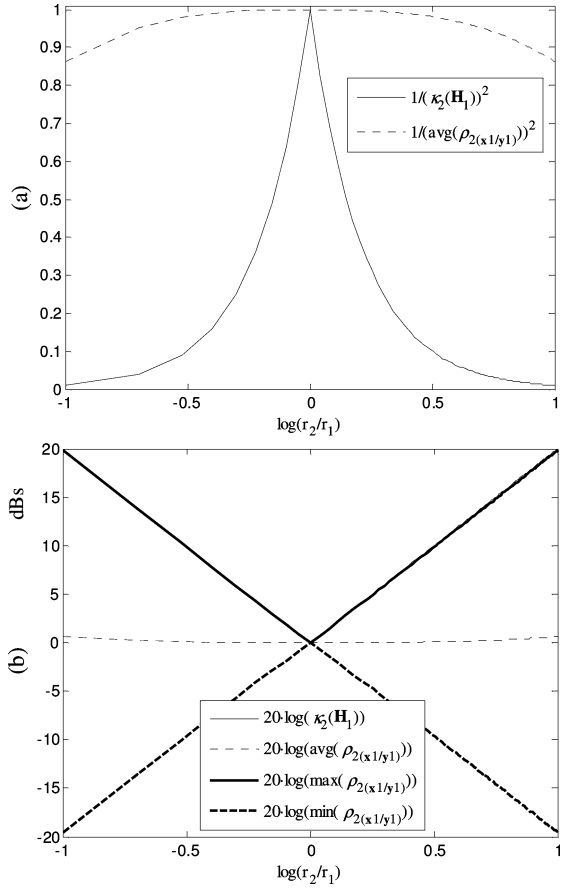

Fig. 10. Error amplification for the differential-drive WMR using *relative error* values for $\mathbf{f}_1$.

In Fig. 9 it is shown the comparison between the error amplification and the maximum theoretical error amplification for the infinity norm: the behavior is qualitatively similar to Fig. 8 and therefore it is concluded that the results obtained for the Euclidean norm can be extrapolated to other norms.

On the other hand, the error values of $\mathbf{f}_1$ considered in (54) are *absolute*, i.e. they do not depend on the velocity values of $\mathbf{y}_1$. For example, this would be the case of an error caused by the encoder resolution when the encoder pulses are used to measure the rotation velocity, or when some electromagnetic noise disturbs a tachometer signal. Nevertheless, the error values of $\mathbf{f}_1$ may also be *relative* to the rotation velocities, e.g. if it is used a tachometer sensor. In this case, for a proportional relationship we have $\mathbf{f}_1 \propto \mathbf{y}_1$. Figure 10 shows the comparison results for a relative error. Note that, in this case the average of the error amplification is much lower. The result is very similar for a wide range of proportionality between $\mathbf{f}_1$ and $\mathbf{y}_1$.

In order to illustrate the importance of the points used to compute the average of the error amplification, it is shown in Fig. 11, two examples with a *non-symmetric* distribution:

$$\text{Fig. 11 (a)} \rightarrow \mathbf{y}_{1\ \text{modified}} = \begin{pmatrix} \dot{\varphi}_1 \\ \dot{\varphi}_2 \end{pmatrix} = \begin{pmatrix} -\dot{\varphi}_{\max} & \cdots & \dot{\varphi}_{\max} \\ -\dot{\varphi}_{\max}/2 & \cdots & \dot{\varphi}_{\max}/2 \end{pmatrix}$$

$$\text{Fig. 11 (b)} \rightarrow \mathbf{f}_{1\ \text{modified}} = \begin{pmatrix} -\dot{\varphi}_{\text{error max}} & \cdots & \dot{\varphi}_{\text{error max}} \\ -\dot{\varphi}_{\text{error max}}/2 & \cdots & \dot{\varphi}_{\text{error max}}/2 \end{pmatrix}. \quad (56)$$

The graphs of Fig. 11 are not symmetric. In particular, the minimum average-error-amplification in Fig. 11(a) is 0.968 and is given by $r_2 = 0.66 \cdot r_1$, in Fig. 11(b) the minimum is 0.937 and is given by $r_2 = 1.905 \cdot r_1$. Both results have a clear physical meaning: (a) if wheel 1 will usually have a higher rotation velocity value than wheel 2, it is preferable (from the error amplification point of view) if it has a higher radius value; (b) if wheel 1 will usually have a higher rotation velocity error than wheel 2, it is preferable if it has a lower radius value. It is conclude that, if there is an a priori knowledge of the usual values for $\{\mathbf{y}_1, \mathbf{f}_1\}$, the optimal values of the WMR parameters (e.g. r_2) may be different from the isotropic ones.

The isotropy and error amplification analysis of the differential-drive WMR consider that the radii of both *fixed* wheels may be different. Obviously, some reasoning, such as {mechanical design (forces distributions), uniformity, common sense, etc.}, suggest that both radii should be equal. Here, it has been mathematically obtained exactly that result but from the error amplification point of view. In other words, this WMR has been used as an illustrative example of the error amplification, and the use of different wheel radii should not be taken as a serious design proposal of this research, although it may have some advantages in specific cases (e.g. Fig. 11).

4.2. WMR with one fixed wheel and one Swedish wheel

In this example it will be considered type II WMR. In particular, it will be analyzed relationship (25) using

https://doi.org/10.1017/S0263574708004165 Published online by Cambridge University Press

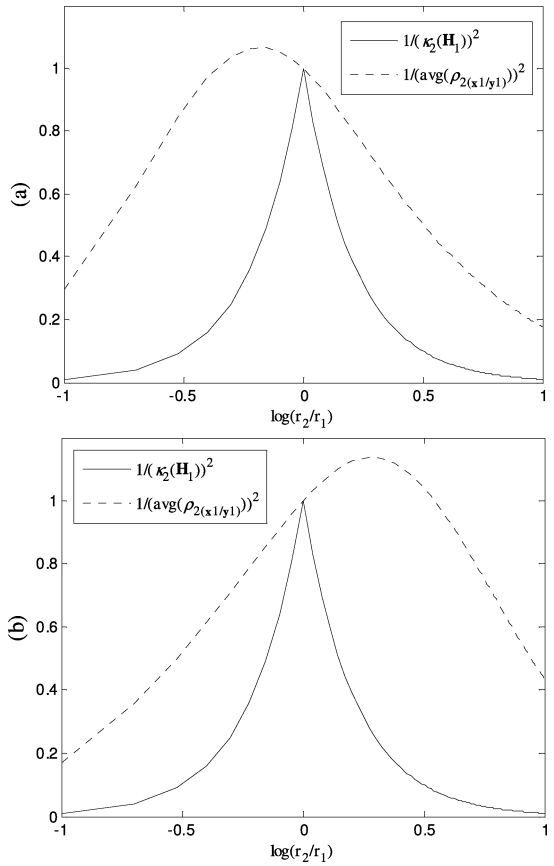

Fig. 11. Error amplification for the differential-drive WMR using a *non-symmetric* set of values for: (a) $\mathbf{y}_{1\ \text{modified}}$, (b) $\mathbf{f}_{1\ \text{modified}}$.

the parameters values $\{r_3 = r_1 = r,\ L = 0,\ \alpha_3 = 90^\circ\}$ and the characteristic length obtained with (29) $\{\beta_{3\ \text{isot}} = \pm 90^\circ, D_2 = l_3\}$:

$$-\frac{1}{r}\begin{pmatrix} 1 & 0 \\ c\beta_3 & s\beta_3 \end{pmatrix}\begin{pmatrix} v_y \\ D_2\omega \end{pmatrix} = \begin{pmatrix} \dot{\varphi}_1 \\ \dot{\varphi}_3 \end{pmatrix} \rightarrow \mathbf{H}_2\ \mathbf{x}_2 = \mathbf{y}_2. \tag{57}$$

Assuming no uncertainty in the angle β_3 of the *Swedish* wheel, i.e. it is a priori known and constant, we have $\mathbf{F}_2 = \mathbf{0}$ and the maximum theoretical relative error amplification is given by the condition number of $\mathbf{H}_2$:

$$\rho_{(\mathbf{x}2/\mathbf{y}2)} \leq \kappa(\mathbf{H}_2) \xrightarrow{\text{e.g.}} \kappa_2(\mathbf{H}_2) = \frac{\max(\sqrt{1 - c\beta_3}, \sqrt{1 + c\beta_3})}{\min(\sqrt{1 - c\beta_3}, \sqrt{1 + c\beta_3})}. \tag{58}$$

In Fig. 12 it is compared the error amplification and the theoretical maximum error amplification (i.e. $\kappa_2(\mathbf{H}_2)$) with respect to angle β_3. Note that isotropy is given by $\beta_3 = \beta_{3\ \text{isot}}$ and β_3 has been *normalized* as $(\beta_3 - \beta_{3\ \text{isot}})/\beta_{3\ \text{isot}}$ (X-axis).

Note that, again the graphs are symmetric with respect to the isotropy condition. It has been verified that the result is very similar, regardless of the use of the absolute or relative error for $\mathbf{f}_2$. As an example, the error amplification for $\beta_3 = 45^\circ$ is:

$$\text{avg}(\rho_{2(\mathbf{x}2/\mathbf{y}2)}) = 1.1173 \qquad \kappa_2(\mathbf{H}_2) = 2.414$$

$$\max(\rho_{2(\mathbf{x}2/\mathbf{y}2)}) = 2.414 \rightarrow \text{for } \left\{ \begin{matrix} \mathbf{y}_2 = (-\dot{\varphi}_{\max}, -\dot{\varphi}_{\max})^{\mathrm{T}} \\ \mathbf{f}_2 = (-\dot{\varphi}_{\text{error max}}, \dot{\varphi}_{\text{error max}})^{\mathrm{T}} \end{matrix} \right\}$$

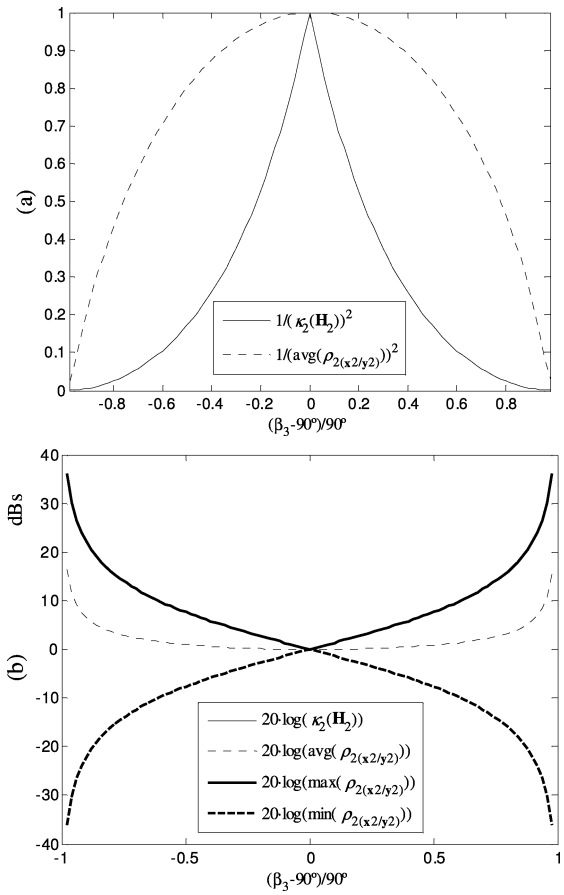

Fig. 12. Error amplification for the WMR with one *fixed* wheel and one *Swedish* wheel.

$$\min(\rho_{2(\mathbf{x}2/\mathbf{y}2)}) = 0.414 \rightarrow \text{for } \{\mathbf{y}_2 = (-\dot{\varphi}_{\max}, \dot{\varphi}_{\max})^{\mathrm{T}}, \mathbf{f}_2 = (\varepsilon, \varepsilon)^{\mathrm{T}}\}. \tag{59}$$

4.3. WMR with one orientable wheel and one Swedish wheel

Here it will be considered type III WMR with *Swedish* wheels (Fig. 6(a)) with the parameter values $\{r_1 = r_2 = r,\ \beta_2 = \alpha_2 = 0^\circ\}$. In particular, it will be analyzed the relationship (from (36)):

$$\frac{1}{r}\begin{pmatrix} 1 & 0 \\ c\beta_1 & -1 \end{pmatrix}\begin{pmatrix} \eta_1 = v_{\mathrm{L}_{y1}} \\ D_7\omega \end{pmatrix} = \begin{pmatrix} \dot{\varphi}_1 \\ \dot{\varphi}_3 \end{pmatrix} \rightarrow \mathbf{H}_3\ \mathbf{x}_3 = \mathbf{y}_3, \tag{60}$$

where η_1 is the forward motion of the WMR in the direction of the *orientable* wheel plane (i.e. L_{y1}), and it has been used the characteristic length from $\{\beta_{1\ \text{isot}} = \pm 90^\circ,\ D_7 = l_2\}$. In this case the angle β_1 of the *orientable* wheel is continuously measured with a sensor and therefore it has some error, i.e. $(\beta_{1\ \text{error}} \neq 0)$. Then, we have $\mathbf{F}_3 \neq \mathbf{0}$ because $\mathbf{H}_3$ depends on β_1.

Figure 13 compares the error amplification and the condition number considering only the error of $\mathbf{H}_3$, i.e. $\{\mathbf{F}_3 \neq \mathbf{0},\ \mathbf{f}_3 = \mathbf{0}\}$. Isotropy is given by $\beta_1 = \beta_{1\ \text{isot}}$ and β_1 has been *normalized* as $(\beta_1 - \beta_{1\ \text{isot}})/\beta_{1\ \text{isot}}$ (X-axis). The graphs are again symmetric with respect to the isotropy condition and the result is the same no matter if it is used absolute or relative error for β_1. Note that in this case (Fig. 13(b)) the maximum error amplification is *lower* than the condition number, meanwhile the minimum error amplification tends to zero ($-80\text{dBs} = 10^{-4}$) and is not in the graph. On the other

https://doi.org/10.1017/S0263574708004165 Published online by Cambridge University Press

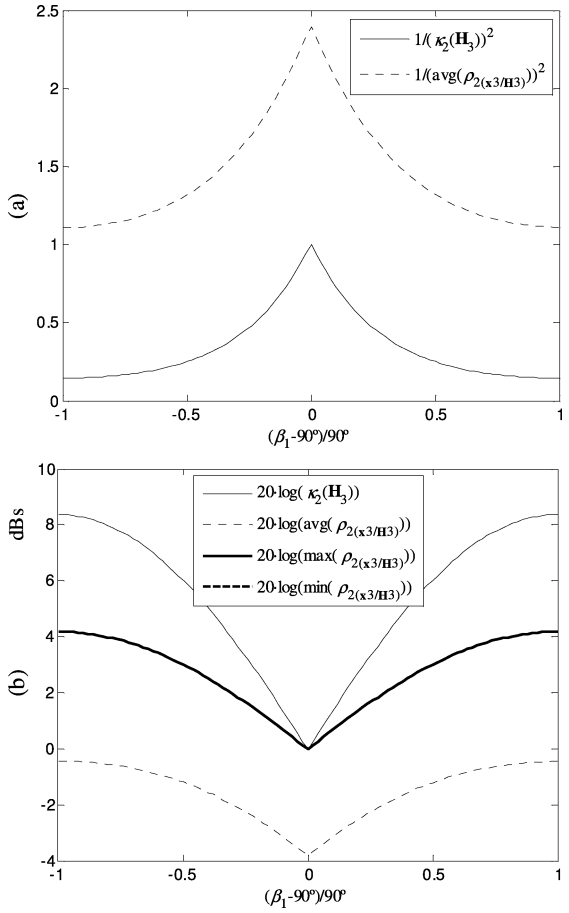

Fig. 13. Error amplification for the WMR with one with one *orientable* wheel and one *Swedish* wheel and $\mathbf{F}_3$ given by $\beta_{1\text{ error}}$.

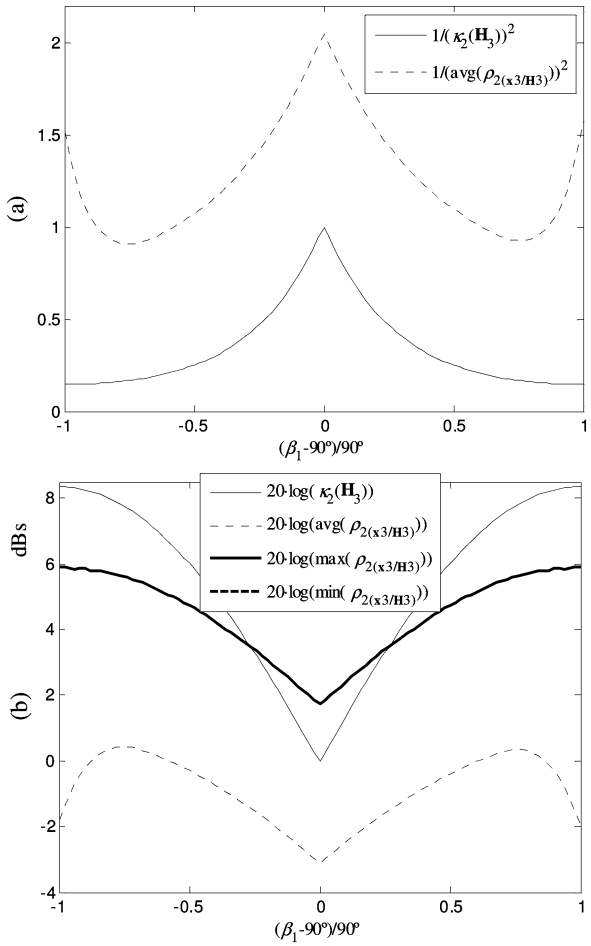

Fig. 14. Error amplification for the WMR with one *orientable* wheel and one *Swedish* wheel and $\mathbf{F}_3$ given by $\beta_{2\text{ error}}$.

hand, if it is considered that the sensor of the *orientable* wheel is very accurate ($\beta_{1\text{ error}} = 0$) and the *Swedish* wheel has some mechanical play that gives rise to angle error ($\beta_{2\text{ error}} \neq 0$), the error matrix $\mathbf{F}_3$ is given by:

$$\in \mathbf{F}_3 = \frac{1}{\mathrm{r}}\left(\begin{pmatrix} 1 & 0 \\ \mathrm{c}(\beta_1 - \beta_{2\text{ error}}) & -\mathrm{c}\beta_{2\text{ error}} \end{pmatrix} - \begin{pmatrix} 1 & 0 \\ \mathrm{c}\beta_1 & -1 \end{pmatrix}\right). \tag{61}$$

Figure 14 shows the new error amplifications for a maximum error of the *Swedish* wheel angle of 10°. As before, the maximum error amplification does not fit the condition number, and for some β_1 values it is higher, see Fig. 14(b). This is produced because the term $O(\in^2)$ (Taylor series expansion of $\mathbf{x}(\in)$ beginning from the second-order term) is not negligible, see (12). The higher is the maximum error of angle β_2, the wider is the range that $\max(\rho_{2(\mathbf{x}3/\mathbf{H}3)}) > \kappa_2(\mathbf{H}_3)$.

5. Conclusion and Further Work

There are several contributions in this research:

– All the kinematic models for the five types of WMRs classified have been obtained. Different to the work of Campion et al[1], these kinematic models include wheel velocity variables, giving straightforward relationships between wheel velocities and WMR velocities, or even mixed.
– A full isotropy characterization has been developed for all the kinematic models of type II and type III WMRs. (Type I has already been tackled in the bibliography[0–8] and isotropy is not applicable for types IV and V.) The specific isotropy conditions represent the optimal setup of wheels in order to avoid relative error amplification and may be used for mechanical design, control applications, motion planning, etc.
– Three illustrative examples have been given to compare the relative error amplification with the condition number or theoretical maximum amplification. The first and second example justify using the isotropy conditions (i.e. the conditions for minimum condition number) in mechanical design, meanwhile the third one justifies to use them in path planning and/or control. It is interesting to remark that, it has been analyzed two important facts that were omitted in previous researches about WMR isotropy[5–9] although they may be very influential in practice. The facts are that the condition number $\kappa(\mathbf{H})$ represents an *upper bound* as long as $O(\in^2)$ (Taylor series expansion of $\mathbf{x}(\in)$ beginning from the second-order term) is null or *negligible*. In particular, the upper bound condition has been verified in the three practical examples of Section 4 and the influence of $O(\in^2)$ has been verified in the third example. It is concluded the two limitations of the isotropy analysis as follows:

https://doi.org/10.1017/S0263574708004165 Published online by Cambridge University Press

- *Condition number limitation due to* $O(\epsilon^2)$: the influence of $O(\epsilon^2)$ may invalidate the upper bound condition of $\kappa(\mathbf{H})$ (condition number), see and Fig. 14(b).
- *Isotropy limitation due to upper bound condition*: if the effect of $O(\epsilon^2)$ is null or negligible (e.g. $\mathbf{F}=0$), the isotropic values of the WMR parameters will be the better choice, i.e. they produce the minimum average-error-amplification, if the WMR matrices and vectors (e.g. $\{\mathbf{y}_1, \mathbf{f}_1\}$ in the example of Section 4.1 are (probabilistically) uniformly and symmetrically distributed. Otherwise, e.g. $\{\mathbf{y}, \mathbf{f}\}$ are not symmetrically distributed or have a unique value (e.g. systematic errors, etc.), the optimal values of the WMR parameters may be different from the isotropic ones (see Fig. 11). Nevertheless, for a specific application it may be difficult to know a priori the probabilistic distributions of the WMR matrices and vectors or if they would be non-uniformly or non-symmetrically distributed. In that case, the isotropic values may be a reasonable choice.

It is suggested as further work to develop a planner that considers the isotropic configurations of a WMR with *orientable* and/or *castor* wheels for path generation. It is also suggested as further work to develop a procedure for mechanical design based on global isotropy for WMRs with *orientable* and/or *castor* wheels. This implies that the WMR parameters (wheel radii, distances between wheels, etc.) would be optimized for minimizing the average condition number across the configuration space.

Acknowledgments

This work was supported in part by the Spanish Government: Research Projects DPI2004-07417-C04-01 and BIA2005-09377-C03-02. The authors would like to thank the anonymous reviewers and Prof. K.H. Low for their valuable comments.

References

1. G. Campion, G. Bastin and B. D'Andrea-Novel, "Structural properties and classification of kinematic and dynamic models of wheeled mobile robots," *IEEE Trans. Rob. Autom.* **12**(1), pp. 47–61 (1996).
2. P. F. Muir and C. P. Neuman, "Kinematic modeling of wheeled mobile robots," *J. Robot. Syst.* **4**(2), pp. 281–329 (1987).
3. J. C. Alexander and J. H. Maddocks, "On the kinematics of wheeled mobile robots," *Int. J. Robot. Res.* **8**(5), pp. 15–27 (1989).
4. L. Gracia and J. Tornero, "A new geometric approach to characterize the singularity of wheeled mobile robots," *Robotica* **25**(5), pp. 627–638 (2007).
5. S. K. Saha, J. Angeles and J. Darcovich, "The design of kinematically isotropic rolling robots with omnidirectional wheels," *Mech. Mach. Theory* **30**(8), pp. 1127–1137 (1995).
6. K. H. Low and Y. P. Leow, "Kinematic modeling, mobility analysis and design of wheeled mobile robots," *Adv. Robotics* **19**, pp. 73–99 (2005).
7. S. Kim and H. Kim, "Isotropy analysis of caster wheeled omnidirectional mobile robot," *Proceedings of the IEEE International Conference on Robotics and Automation*, New Orleans, USA (2004) pp. 3093–3098.
8. S. Kim, H. Kim and B. Moon, "Local and global isotropy of caster wheeled omnidirectional mobile robots," *Proceedings of the IEEE International Conference on Robotics and Automation*, Barcelona, Spain (2005) pp. 3457–3462.
9. S. Kim, B. Moon and I. Jung, "Optimal isotropic characteristics of caster wheeled omnidirectional mobile robot," *Proceedings of the IEEE/RSJ International Conference on Intelligent Robots and Systems*, Beijing, China (2006) pp. 5576–5581.
10. G. H. Golub and C. F. Van Loan, *Matrix Computations* (The Johns Hopkins University Press, 3rd ed. Baltimore, 1996), pp. 80, 242.
11. N. J. Higham, *Accuracy and Stability of Numerical Algorithms* (SIAM Publications, Philadelphia, 1996), ch. 7, 20, 21.
12. H. Lipkin and J. Duffy, "Hybrid twist and wrench control for a robotic manipulator," *ASME J. Mech. Transm. Autom. Des.* **110**, pp. 138–144 (1988).
13. M. Tandirci, J. Angeles and F. Ranjbaran, "The characteristic point and the characteristic length of robotic manipulators," *Proceedings. of the ASME 22nd Biennial Mechanisms Conference*, Arizona (1992) **45**, pp. 203–208.
14. O. Ma and J. Angeles, "Optimum architecture design of platform manipulators," *Proceedings of the IEEE International Conference on Advanced Robotics*, Pisa, Italy (1991) pp. 1131–1135.
15. L. Stocco, S. E. Salcudean and F. Sassani, "Matrix normalization for optimal robot design," *Proceedings of the IEEE International Conference on Robotics and Automation*, Leuven, Belgium (1998) **2**, pp. 1346–1351.
16. L. J. Stocco, S. E. Salcudean and F. Sassani, "On the use of scaling matrices for task-specific robot design," *IEEE Trans. Robot. Autom.* **15**(5), pp. 958–965 (1999).

https://doi.org/10.1017/S0263574708004165 Published online by Cambridge University Press